

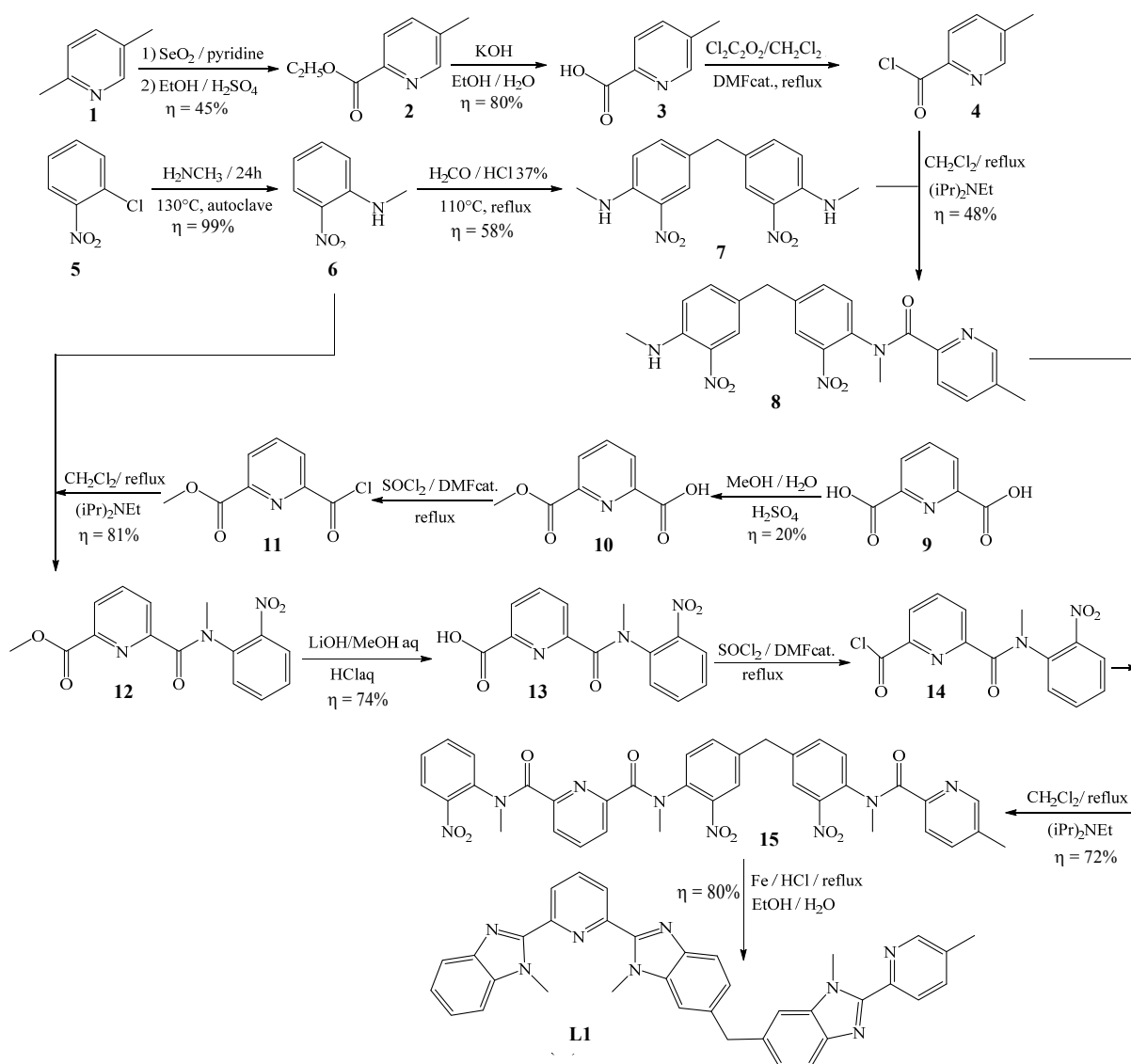
**Smaller than a nanoparticles with the design of discrete polynuclear molecular complexes displaying NIR to VIS upconversion.**

---

Davood Zare, Yan Suffren, Laure Guénée, Svetlana V. Eliseeva, Homayoun Nozary, Lilit Aboshyan-Sorgho, Stéphane Petoud,<sup>\*</sup> Andreas Hauser,<sup>\*</sup> and Claude Piguet<sup>\*</sup>

**Supporting Information** (40 pages)

## Appendix 1. Synthesis of ligand L1



**Scheme A1-1** Multi-step synthesis of ligand L1

**Preparation of 5-methyl-2-pyridinecarboxylic acid-ethyl ester (2).** 2,5-lutidine (**1**, 10.0 g, 93.3 mmol) and selenium dioxide (15.54 g, 111 mmol) were dissolved in pyridine (60 mL) and refluxed for 36 h under an inert atmosphere. The mixture was cooled to room temperature and filtered. The residual solid was washed successively with pyridine (60 mL) and distilled water (60 mL). In order to get rid of residual pyridine, water (300 mL) was added to and the resulting mixture was distilled under vacuum. This procedure was repeated several times till no trace of pyridine remained (TLC). The resulting solution was filtered over cellulose and evaporated to dryness under vacuum (80°C,

$\sim 10^{-2}$  Torr). The residue was suspended in ethanol (400 mL), concentrated  $\text{H}_2\text{SO}_4$  (8 mL) was added and the resulting mixture was refluxed for 15h under an inert atmosphere ( $\text{N}_2$ ). After cooling at RT, water (50 mL) was added and the mixture was neutralized ( $\text{pH} = 7$ ) with aqueous NaOH (5M). Ethanol was removed by evaporation and the aqueous phase was extracted with dichloromethane ( $3 \times 100$  mL). The combined organic fractions ( $3 \times 100$  mL) were dried ( $\text{Na}_2\text{SO}_4$ ), evaporated and the residual oil distilled ( $90^\circ\text{C}$ ,  $\sim 10^{-2}$  Torr) to give 6.936 g of **2** as a colorless liquid (41.99 mmol, yield 45%).

$^1\text{H}$  NMR ( $\text{CDCl}_3$ , 400MHz)  $\delta/\text{ppm}$ : 8.57 (q,  $^4J = 0.8$  Hz, 1H), 8.03 (d,  $^3J = 8.0$  Hz, 1H), 7.61 (dq,  $^3J = 8.0$  Hz,  $^4J = 0.8$  Hz, 1H), 4.46 (d,  $^3J = 7.2$  Hz, 2H), 2.41 (s, 3H), 1.44 (t,  $^3J = 7.2$  Hz, 3H). ESI-MS ( $\text{CH}_2\text{Cl}_2/\text{MeOH}$ )  $m/z$ : 166.4 ( $[\text{M}+\text{H}]^+$ ), 188.4 ( $[\text{M}+\text{Na}]^+$ ).

**Preparation of 5-methyl-2-pyridinecarboxylic acid (3).** 5-Methyl-2-pyridinecarboxylic acid-ethyl ester (**2**, 5.00 g, 30.27 mmol) were dissolved in ethanol (150 mL) and aq. KOH (9.16 g in 150 mL water). The mixture was refluxed for 1 hour, ethanol was removed by evaporation and the aq. phase extracted with dichloromethane ( $3 \times 50$  mL). The aqueous phase was acidified with HCl to  $\text{pH} = 3.5$  and evaporated to dryness under vacuum. The residual solid was dissolved in 700 mL of ethylacetate, refluxed for 3 h and filtered while hot on a Büchner. The volume of the filtrate was reduced by rotatory evaporation until precipitation took place. After cooling at  $-20^\circ\text{C}$  for 12 h, the precipitate was separated by filtration. The volume of the remaining organic phase was again reduced, cooled and filtered and this procedure was repeated several times to give 3.32 g of **3** (24.22 mmol, yield 80%) as a white solid.

$^1\text{H}$  NMR ( $\text{CDCl}_3$ , 400MHz)  $\delta/\text{ppm}$ : 8.50 (s, 1H), 8.14 (d,  $^3J = 8.0$  Hz, 1H), 7.76 (dq,  $^3J = 8.0$  Hz,  $^4J = 0.8$  Hz, 1H), 2.47 (s, 3H). ESI-MS ( $\text{CHCl}_3$ )  $m/z$ : 136.1 ( $[\text{M}-\text{H}]^-$ ).

**Preparation of *N*-methyl-2-nitro-aniline (6).** Ortho-chloronitrobenzene (**5**, 10.00 g, 63 mmol) and methylamine (40% in water, 65.3 mL) were heated in an autoclave at  $130^\circ\text{C}$  for 24 h. The dark mixture was evaporated to dryness, partitioned between dichloromethane (50 mL) and half-sat. aq.

NH<sub>4</sub>Cl (50 mL), extracted with dichloromethane (2×50 mL). The combined organic phases were dried (Na<sub>2</sub>SO<sub>4</sub>), evaporated to dryness and the crude product purified by column chromatography (Silicagel; CH<sub>2</sub>Cl<sub>2</sub>/Hexane 80:20) to give 9.52 g of **6** (62.9 mmol, yield 99%) as a dark orange solid.

<sup>1</sup>H NMR (CDCl<sub>3</sub>, 400MHz) δ/ppm: 8.17 (dd, 1H, <sup>3</sup>J = 8.8 Hz, <sup>4</sup>J = 1.6 Hz, 1H), 8.03 (s, br, 1H), 7.46 (tdd, <sup>3</sup>J = 8.0 Hz, <sup>4</sup>J = 1.6 Hz, <sup>5</sup>J = 0.6 Hz, 1H), 6.84 (dd, <sup>3</sup>J = 8.8 Hz, <sup>4</sup>J = 0.8 Hz, 1H), 6.65 (td, <sup>3</sup>J = 8.0 Hz, <sup>4</sup>J = 1.2 Hz, 1H), 3.02 (d, <sup>3</sup>J = 4.8 Hz, 3H). ESI-MS (CH<sub>2</sub>Cl<sub>2</sub>/MeOH) *m/z*: 152.4 ([M+H]<sup>+</sup>).

**Preparation of 4,4'-methylene-2,2'-dinitro-bis(*N*-methyl-aniline) (7).**

*N*-methyl-2-nitro-aniline (**6**, 10 g, 60.25 mmol), paraformaldehyde (0.909 g, 30.13 mmol) and concentrated HCl (37%, 100 mL) were mixed and heated progressively: 1h at 40°C, 1h at 60 °C, 12 h at 120 °C. After cooling the mixture at room temperature, water (380 mL) was added and the excess of acid was neutralized to pH = 9 with 24% aq. NH<sub>4</sub>OH. The resulting mixture was extracted with dichloromethane (3 × 100 mL). The combined organic layers were dried (Na<sub>2</sub>SO<sub>4</sub>), evaporated to dryness and the crude product purified by column chromatography (Silicagel; CH<sub>2</sub>Cl<sub>2</sub> 100%) to give 5.45 g of **7** as a red powder (17.34 mmol, yield 58%).

<sup>1</sup>H NMR (CDCl<sub>3</sub>, 400MHz) δ/ppm: 8.00 (s, 2H), 7.29 (d, <sup>3</sup>J = 1.6 Hz, 2H), 6.80 (d, <sup>3</sup>J = 8.0 Hz, 2H), 3.81 (s, 2H), 3.01 (s, 6H). ESI-MS (CH<sub>2</sub>Cl<sub>2</sub>/MeOH) *m/z*: 317 ([M+H]<sup>+</sup>), 331 ([M+NH<sub>4</sub>]<sup>+</sup>), 633 ([2M+H]<sup>+</sup>).

**Preparation of *N*,5-dimethyl-*N*-{4'-[4''-(methylamino)-3''-nitrobenzyl]-2'-nitrophenyl} pyridine-2-carboxamide (8).** 5-Methyl-2-pyridinecarboxylic acid (**3**, 1.45 g, 10.57 mmol) and DMF (100 μL) were refluxed in oxalyl chloride (2M in CH<sub>2</sub>Cl<sub>2</sub>, 53 mL) for 45 min. Excess oxalyl chloride was distilled from the reaction mixture, which was then co-evaporated with dry dichloromethane (2 × 20 mL), then dried under vacuum. The resulting solid **4** was solubilized in dry dichloromethane (60 mL) and added dropwise into a dry dichloromethane (100 mL) solution of

4,4'-methylene-2,2'-dinitro-bis(*N*-methyl-aniline) (**7**, 9.98 g, 31.5 mmol). The resulting mixture was refluxed under an inert atmosphere, the reaction was followed by TLC while the pH was kept in the 7-8 range by the progressive addition of di-isopropylethylamine. After 12 h, the resulting mixture was evaporated to dryness, partitioned between dichloromethane (150 mL) and half-sat. aq. NH<sub>4</sub>Cl (100 mL). The organic phase was separated and the remaining aqueous phase was extracted with dichloromethane (3 × 30 mL). The combined organic fractions were dried over Na<sub>2</sub>SO<sub>4</sub>, evaporated to dryness and the crude product purified by column chromatography (Silicagel; CH<sub>2</sub>Cl<sub>2</sub>/MeOH 100:0 → 99:1) to give 2.15 g of **8** (5 mmol, yield 48%).

<sup>1</sup>H NMR (CDCl<sub>3</sub>, 400MHz) δ/ppm: 8.02 (m, 1H), 7.95-7.85 (m, 2H), 7.68-7.66 (m, 2H), 7.44 (d, <sup>3</sup>J = 8 Hz, 1H), 7.32-7.23 (m, 3H), 6.83 (d, <sup>3</sup>J = 8.4 Hz, 1H), 4.00-3.93 (m, 2H), 3.50-3.47 (m, 3H), 3.03 (d, <sup>3</sup>J = 4.8 Hz, 3H), 2.41-2.24 (m, 3H). ESI-MS (CH<sub>2</sub>Cl<sub>2</sub>/MeOH) *m/z*: 436 ([M+H]<sup>+</sup>), 458 ([M+Na]<sup>+</sup>), 871 ([2M+H]<sup>+</sup>).

**Preparation of pyridine-2,6-dicarboxylic acid-monomethyl ester (10).** Pyridine-2,6-dicarboxylic acid 10.26 g, (**9**, 61.4 mmol), methanol (50 mL), water (50 mL) and concentrated H<sub>2</sub>SO<sub>4</sub> (5 mL) were refluxed until the solid was completely dissolved (30 min). The reaction mixture was cooled and neutralized with aq. sat. NaHCO<sub>3</sub> (300 mL). Methanol was removed by rotatory evaporation and the aq. phase was extracted with dichloromethane (3 × 30 mL) for removing the unwanted di-ester product. The aqueous phase was acidified with concentrated HCl (37%) to pH = 2 and filtered for removing solid pyridine-2,6-dicarboxylic acid. The aq. filtrate was extracted with dichloromethane (4 × 50 mL) and evaporated to dryness to give 2.25 g of **10** (12.43 mmol, yield 20 %).

<sup>1</sup>H NMR (CDCl<sub>3</sub>, 400MHz) δ/ppm: 8.42 (d, 1H, <sup>3</sup>J = 8.0 Hz), 8.35 (d, 1H, <sup>3</sup>J = 8.0 Hz), 8.12 (t, 1H, <sup>3</sup>J = 8.0 Hz), 4.04 (s, 3H). ESI-MS (CHCl<sub>3</sub>) *m/z*: 180 ([M-H]<sup>-</sup>).

**Preparation of 6-[methyl(2-nitrophenyl)carbamoyl]pyridine-2-carboxylic acid methylester (12).** Pyridine-2,6-dicarboxylic acid-monomethyl ester (**10**, 2 g, 11 mmol) and DMF (100 μl) were

refluxed in thionyl chloride (24 mL) for 1h. Excess thionyl chloride was distilled from the reaction mixture, which was then co-evaporated with dry dichloromethane (3×25 mL) and dried under vacuum. The solid **11** was solubilized in dry dichloromethane (50 mL) and added dropwise into a dry dichloromethane (100 mL) solution of *N*-methyl-2-nitro-aniline (**6**, 1.67 g, 11 mmol). The resulting mixture was refluxed under an inert atmosphere, the reaction was followed by TLC while the pH was kept in the 7-8 range by the progressive addition of di-isopropylethylamine. After 12 h, the resulting mixture was evaporated to dryness, partitioned between dichloromethane (150 mL) and half-sat. aq. NH<sub>4</sub>Cl (100 mL). The organic phase was separated and the aq. phase was extracted with dichloromethane (3 × 50 mL). The combined organic fractions were dried over Na<sub>2</sub>SO<sub>4</sub>, evaporated to dryness and the crude product purified by column chromatography (Silicagel; CH<sub>2</sub>Cl<sub>2</sub>/MeOH 100:0 → 98.5:1.5) to give 2.83 g of **12** (8.97 mmol, yield 81%).

<sup>1</sup>H NMR (CDCl<sub>3</sub>, 400MHz) δ/ppm: 8.07 (dd, <sup>3</sup>J = 8.0Hz, <sup>4</sup>J = 0.8 Hz, 1H), 8.01 (dt, <sup>3</sup>J = 8.0Hz, <sup>4</sup>J = 0.8 Hz, 1H), 7.96 (dd, <sup>3</sup>J = 8.0Hz, <sup>4</sup>J = 0.8 Hz, 1H), 7.84 (t, <sup>3</sup>J = 8.0Hz, 1H), 7.56 (td, <sup>3</sup>J = 8.0Hz, <sup>4</sup>J = 0.8 Hz, 1H), 7.39 (m, 2H), 3.83 (s, 3H), 3.53(s, 3H). ESI-MS (CH<sub>2</sub>Cl<sub>2</sub>/MeOH) *m/z*: 316 ([M+H]<sup>+</sup>), 333 ([M+NH<sub>4</sub>]<sup>+</sup>), 338 ([M+Na]<sup>+</sup>), 631 ([2M+H]<sup>+</sup>), 648 ([2M+NH<sub>4</sub>]<sup>+</sup>).

**Preparation of 6-[methyl(2-nitrophenyl)carbamoyl]pyridine-2-carboxylic acid (13).** A solution of LiOH (1.893 g, 45 mmol) in water (30 mL) was dropwise added into a cooled (0 °C) solution of 6-[methyl(2-nitrophenyl)carbamoyl]pyridine-2-carboxylic acid methylester (**12**, 2.83 g, 8.97 mmol) in methanol (50 mL). The resulting mixture was stirred at 0 °C for 1.5-2 h, poured into water (600 mL) and washed with dichloromethane (4 × 100 mL). The aqueous phase was acidified at pH = 2 with conc. hydrochloric acid, and extracted with dichloromethane (4 × 100 mL). The combined organic phases were dried over Na<sub>2</sub>SO<sub>4</sub>, filtered and evaporated to dryness. The crude residue was purified by column chromatography (Silicagel, CH<sub>2</sub>Cl<sub>2</sub>:CH<sub>3</sub>OH = 100:0→98.5:1.5) to give **13** as a yellow solid (2 g, 6.64 mmol, yield 74%).

$^1\text{H}$  NMR ( $\text{CDCl}_3$ , 400MHz,  $\delta$  ppm): 8.18 (dd,  $^3J = 7.6$  Hz,  $^4J = 1.1$  Hz, 1H), 8.13 (dd,  $^3J = 8$  Hz,  $^4J = 1.2$  Hz, 1H), 8.00 (t,  $^3J = 8$  Hz, 1H), 7.78 (dd,  $^3J = 8$  Hz,  $^4J = 1.6$  Hz, 1H), 7.63 (dd,  $^3J = 8.4$  Hz,  $^4J = 1.2$  Hz, 1H), 7.48 (td,  $^3J = 8$  Hz,  $^4J = 1.2$  Hz, 1H), 7.41 (dd,  $^3J = 8$  Hz,  $^4J = 1.2$  Hz, 1H), 3.56 (s, 3H). ESI-MS ( $\text{CHCl}_3$ )  $m/z$ : 300 ( $[(\text{M}-\text{H})^-]$ ), 601.3 ( $[2\text{M}-\text{H}]^-$ ).

**Preparation of 6-[1'''-(*N*-methyl-*N*-carbamoyl-2-nitroaniline)]-*N*-methyl-*N*-{4'-{4''-{*N*-methyl-*N*-[(5'''-methylpyridin-2''-yl)carbonyl]amino}-3''-nitrobenzyl]-2'-**

**nitrophenyl}pyridine-2-carboxamide (15).** 6-[methyl(2-nitrophenyl)carbamoyl]pyridine-2-carboxylic acid (**13**, 1g, 3.32mmol) and DMF (200  $\mu\text{l}$ ) were refluxed in thionyl chloride (10 mL) for 1h. Excess thionyl chloride was distilled from the reaction mixture, which was then co-evaporated with dry dichloromethane (3 $\times$ 30 mL) and dried under vacuum. The solid **14** was solubilized in dry dichloromethane (50 mL) and dropwise added into a dry dichloromethane (100 mL) solution of *N*,5-dimethyl-*N*-{4'-[4''-(methylamino)-3''-nitrobenzyl]-2'-nitrophenyl} pyridine-2-carboxamide (**8**, 1.443 g, 3.32 mmol). The resulting mixture was refluxed under an inert atmosphere and the reaction was followed by TLC while the pH was kept in the 7-8 range by the progressive addition of di-isopropylethylamine. After 18 h, the resulting mixture was evaporated to dryness, partitioned between dichloromethane (150 mL) and half-sat. aq.  $\text{NH}_4\text{Cl}$  (100 mL). The organic phase was separated and the aq. phase was extracted with dichloromethane (3  $\times$  30 mL). The combined organic fractions were dried over  $\text{Na}_2\text{SO}_4$ , evaporated to dryness and the crude product purified by column chromatography (Silicagel;  $\text{CH}_2\text{Cl}_2/\text{MeOH}$  100:0  $\rightarrow$  98:2) to give 1.723 g of **15** (2.4 mmol, yield 72%).

$^1\text{H}$  NMR (DMSO, 400MHz)  $\delta$ /ppm: 8.05-8.21 (m, 2H), 7.83-8.02 (m, 3H), 7.58-7.77 (m, 2H), 7.48-7.57 (m, 2H), 7.33-7.47 (m, 4H), 7.08 (d,  $^3J = 7.6$  Hz, 1H), 6.92-7.02 (m, 2H), 3.97 (s, 2H), 3.36 (s, 3H), 2.94 (s, 3H), 1.95 (s, 3H), 1.23 (s, 3H). ESI-MS ( $\text{CH}_2\text{Cl}_2/\text{MeOH}$ )  $m/z$ : 719 ( $[\text{M}+\text{H}]^+$ ), 1437 ( $[2\text{M}+\text{H}]^+$ ).

**Preparation of 2-{6-[1-(methyl)-1H-benzimidazol-2-yl]pyridin-2-yl}-1,1'-dimethyl-5,5'-methylene-2'-(5-methylpyridin-2-yl)bis[1H-benzimidazole] (L1).** Compound **15** (1.2 g, 1.67 mmol, 1 eq) was dissolved in ethanol/water (120 mL: 30 mL). Activated iron powder (5.6 g, 100 mmol, 60 eq) and concentrated hydrochloric acid (37%, 4.1 mL, 49.87mmol) were added and the mixture refluxed for 25 h. The excess of iron was removed by using a magnetic stick and ethanol was distilled under vacuum. The resulting mixture was poured into CH<sub>2</sub>Cl<sub>2</sub> (300 mL), Na<sub>2</sub>H<sub>2</sub>EDTA·2H<sub>2</sub>O (48 g) dissolved in water (350 mL) was added and the resulting stirred mixture was neutralized (pH=8.5) with 24% aq. NH<sub>4</sub>OH concentrated hydrogen peroxide (30%, 22.7 mL) was added under vigorous stirring. After 45 minutes, the organic layer was separated and the aqueous phase extracted with CH<sub>2</sub>Cl<sub>2</sub> (4 × 50 mL). The combined organic phases were dried (Na<sub>2</sub>SO<sub>4</sub>), evaporated to dryness and the crude residue purified by column chromatography (Silicagel; CH<sub>2</sub>Cl<sub>2</sub>/MeOH 99.9:0.1→97:3) and crystallized from dichloromethane/hexane to give 920 mg (0.16 mmol, yield 80%) of the final ligand **L1** as a pale cream powder.

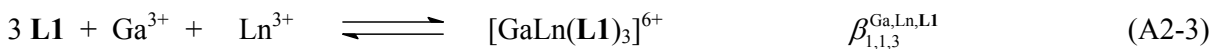
<sup>1</sup>H NMR (CDCl<sub>3</sub>, 400MHz) δ/ppm: 8.54 (q, <sup>4</sup>J = 0.8 Hz, 1H), 8.43 (s, 1H), 8.41 (s, 1H), 8.28 (d, <sup>3</sup>J = 8.0 Hz, 1H), 8.05 (td, <sup>3</sup>J = 8.0 Hz, <sup>5</sup>J = 0.16 Hz, 1H), 7.89 (dd, <sup>3</sup>J = 8.0 Hz, <sup>4</sup>J = 4 Hz, 1H), 7.77 (d, <sup>4</sup>J = 0.8 Hz, 1H), 7.72 (d, <sup>5</sup>J = 0.8 Hz, 1H), 7.65 (ddd, <sup>3</sup>J = 8 Hz, <sup>4</sup>J = 4 Hz, <sup>5</sup>J = 0.8 Hz, 1H), 7.48 (dd, <sup>3</sup>J = 8 Hz, <sup>4</sup>J = 2 Hz, 1H), 7.34 (m, 4H), 7.29 (d, <sup>3</sup>J = 8.0 Hz, 1H), 7.23 (td, <sup>3</sup>J = 8.0 Hz, <sup>4</sup>J = 1.6 Hz, 1H), 4.32 (s, 2H), 4.26 (s, 3H), 4.25 (s, 3H), 4.23 (s, 3H), 2.43 (s, 3H). ESI-MS (CH<sub>2</sub>Cl<sub>2</sub>/MeOH) *m/z*: 575.2 ([M+H]<sup>+</sup>), 1150.4 ([2M+H]<sup>+</sup>). Elemental analysis for C<sub>36</sub>H<sub>30</sub>N<sub>8</sub>·0.15CH<sub>2</sub>Cl<sub>2</sub>; calcd: %C 73.90, %H 5.20, %N 19.06; found %C 74.00, %H 5.25, %N 18.68.

## Appendix 2. Determination of the thermodynamic exchange constant for $[\text{GaLn}(\text{L1})_3]^{6+}$ in solution.

The  $^1\text{H}$  NMR spectrum recorded at equilibrium for reaction (A2-1) showed the coexistence of  $[\text{GaY}(\text{L1})_3]^{6+}$  and  $[\text{GaEu}(\text{L1})_3]^{6+}$  (Figure S4), from which the thermodynamic exchange constant can be written as eq. (A2-2).  $[\text{GaLn}]_{\text{eq}}$ ,  $[\text{Ln}]_{\text{eq}}$  and  $[\text{L1}]_{\text{eq}}$  correspond to the equilibrium concentrations of the complexes, free metals and free ligand, respectively and  $c^\theta = 1.0 \text{ M}$  stands for the concentration of the reference state. The cumulative formation constants  $\beta_{1,1,3}^{\text{Ga,Ln,L1}}$  are defined in eqs (A2-3)-(A2-4).



$$K_{\text{exch}}^{\text{Y,Eu}} = \frac{\beta_{1,1,3}^{\text{Ga,Eu,L1}}}{\beta_{1,1,3}^{\text{Ga,Y,L1}}} = \frac{([\text{GaEu}]_{\text{eq}}/c^\theta)([\text{Y}]_{\text{eq}}/c^\theta)}{([\text{GaY}]_{\text{eq}}/c^\theta)([\text{Eu}]_{\text{eq}}/c^\theta)} \quad (\text{A2-2})$$



$$\beta_{1,1,3}^{\text{Ga,Ln,L1}} = \frac{([\text{GaLn}]_{\text{eq}}/c^\theta)}{([\text{Ga}]_{\text{eq}}/c^\theta)([\text{Ln}]_{\text{eq}}/c^\theta)([\text{L1}]_{\text{eq}}/c^\theta)^3} \quad (\text{A2-4})$$

Integrating the signal of the same proton in  $[\text{GaY}(\text{L1})_3]^{6+}$  ( $I_{\text{GaY}}$ ) and in  $[\text{GaEu}(\text{L1})_3]^{6+}$  ( $I_{\text{GaEu}}$ ) gives

$$\frac{I_{\text{GaEu}}}{I_{\text{GaY}}} = \frac{[\text{GaEu}]_{\text{eq}}}{[\text{GaY}]_{\text{eq}}} \quad (\text{A2-5})$$

while the mass balances for Eu, Y and Ga yields

$$[\text{Y}]_{\text{tot}} = [\text{Y}]_{\text{eq}} + [\text{GaY}]_{\text{eq}} \quad (\text{A2-6})$$

$$[\text{Eu}]_{\text{tot}} = [\text{Eu}]_{\text{eq}} + [\text{GaEu}]_{\text{eq}} \quad (\text{A2-7})$$

$$[\text{Ga}]_{\text{tot}} = [\text{GaY}]_{\text{eq}} + [\text{GaEu}]_{\text{eq}} \quad (\text{A2-8})$$

The introduction of eq. (A2-5) into eq. (A2-8) leads to

$$[\text{GaEu}]_{\text{eq}} = \frac{I_{\text{GaEu}}}{I_{\text{GaEu}} + I_{\text{GaY}}} [\text{Ga}]_{\text{tot}} \quad \text{and} \quad [\text{GaY}]_{\text{eq}} = \frac{I_{\text{GaY}}}{I_{\text{GaEu}} + I_{\text{GaY}}} [\text{Ga}]_{\text{tot}} \quad (\text{A2-9})$$

Combination of eqs (A2-6) and (A2-7) with (A2-9) provides

$$\frac{[Y]_{\text{eq}}}{[Eu]_{\text{eq}}} = \frac{(I_{\text{GaEu}} + I_{\text{GaY}})[Y]_{\text{tot}} - I_{\text{GaY}}[Ga]_{\text{tot}}}{(I_{\text{GaEu}} + I_{\text{GaY}})[Eu]_{\text{tot}} - I_{\text{GaEu}}[Ga]_{\text{tot}}} \quad (\text{A2-10})$$

Introducing Eqs (A2-5) and (A2-10) into (A2-2) eventually yields

$$K_{\text{exch}}^{Y,\text{Eu}} = \frac{I_{\text{GaEu}}}{I_{\text{GaY}}} \cdot \left[ \frac{(I_{\text{GaEu}} + I_{\text{GaY}})[Y]_{\text{tot}} - I_{\text{GaY}}[Ga]_{\text{tot}}}{(I_{\text{GaEu}} + I_{\text{GaY}})[Eu]_{\text{tot}} - I_{\text{GaEu}}[Ga]_{\text{tot}}} \right] \quad (\text{A2-11})$$

which is used for estimating the exchange constant from the integration of the  $^1\text{H}$  NMR spectrum.

### Appendix 3. Kinetic analysis of the exchange process affecting $[\text{GaLn}(\text{L1})_3]^{6+}$ in solution.

The time evolution of the  $^1\text{H}$  NMR spectra recorded upon reaction of  $[\text{GaY}(\text{L1})_3]^{6+}$  with  $\text{Eu}(\text{CF}_3\text{SO}_3)_3$  in solution showed the exclusive replacement of  $[\text{GaY}(\text{L1})_3]^{6+}$  with  $[\text{GaEu}(\text{L1})_3]^{6+}$  without accumulation of any intermediate complex in significant amount (Figure S4). Considering reaction (A2-1) as a reversible second-order reaction, the associated reaction rate  $V$  is given in eq. (A3-1) where  $k_f$  and  $k_r$  stand for the forward, respectively backward second-order rate constants.

$$V = -\frac{d[\text{GaY}]}{dt} = k_f [\text{GaY}][\text{Eu}] - k_r [\text{GaEu}][\text{Y}] \quad (\text{A3-1})$$

The introduction of the mass balances eqs (A2-6) to (A2-8) followed by straightforward algebraic rearrangement give

$$-\frac{d[\text{GaY}]}{dt} = [\text{GaY}]^2 (k_f - k_r) + [\text{GaY}] \{ k_f ([\text{Eu}]_{\text{tot}} - [\text{Ga}]_{\text{tot}}) + k_r ([\text{Y}]_{\text{tot}} + [\text{Ga}]_{\text{tot}}) \} - k_r [\text{Ga}]_{\text{tot}} [\text{Y}]_{\text{tot}} \quad (\text{A3-2})$$

The analytical integration of this differential equation can be found in reference 16.

Derivation of the kinetic trace recorded for  $[\text{GaY}(\text{L1})_3]^{6+}$  (Figure 2) provides pseudo-linear  $V = -d[\text{GaY}]/dt$  versus  $[\text{GaY}]$  plots (Figure A3-1) reminiscent to a reversible pseudo-first-order reversible reaction mechanism (see main text).<sup>17</sup>

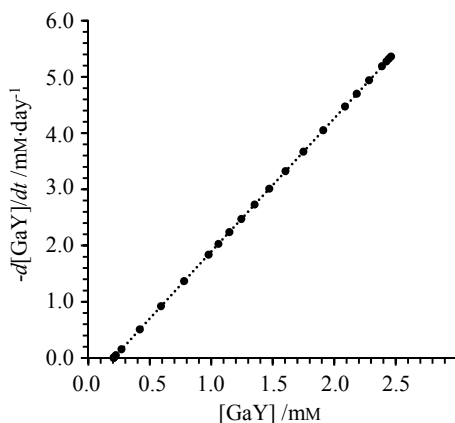


**Figure A3-1** Derivative of the kinetic trace monitored by  $^1\text{H}$  NMR for the reaction of  $[\text{GaY}(\text{L1})_3](\text{CF}_3\text{SO}_3)_6$  (1.0 eq) with  $\text{Eu}(\text{CF}_3\text{SO}_3)_3$  (1.0 eq) at 293 K. The dotted lines correspond to the best linear fit.

#### Appendix 4: Calculation of normalized steady-state population densities in molecular systems.

The dynamic behavior of any molecular system  $S_nA_m$  containing a discrete number of activators (A) and sensitizers (S) can be modeled with a set of linear differential equations written in the matrix form<sup>17</sup>

$$\left[ \frac{dN^{(i)}}{dt} \right] = \mathbf{M} \times [N^{(i)}] \quad (\text{A4-1})$$

$\mathbf{M}$  depends on the kinetic diagram and corresponds to

$$\mathbf{M} = \begin{pmatrix} -k_A^{\text{exc}(0 \rightarrow 1)} & k_A^{1 \rightarrow 0} & k_A^{2 \rightarrow 0} \\ k_A^{\text{exc}(0 \rightarrow 1)} & -(k_A^{1 \rightarrow 0} + k_A^{\text{exc}(1 \rightarrow 2)}) & k_A^{2 \rightarrow 1} \\ 0 & k_A^{\text{exc}(1 \rightarrow 2)} & -(k_A^{2 \rightarrow 0} + k_A^{2 \rightarrow 1}) \end{pmatrix} \quad \text{for the simple one ion ESA mechanism}$$

depicted in Scheme 2a. Under steady-state conditions, eq. (A4-1) becomes

$$\mathbf{M} \times [N^{(i)}] = [0] \quad (\text{A4-2})$$

However, mass conservation within the kinetic diagram implies that  $\mathbf{M}$  is singular (*i.e.*  $\det(\mathbf{M}) = 0$ ) and the lack of an inverse matrix precludes a non-trivial solution for eq. A4-2. The missing information is contained in the mass balance (eq. A4-3), which is added as an additional line in the kinetic matrix transforming  $\mathbf{M}$  into its rectangular form  $\mathbf{M}'$

$$\begin{pmatrix} -k_A^{\text{exc}(0 \rightarrow 1)} & k_A^{1 \rightarrow 0} & k_A^{2 \rightarrow 0} \\ k_A^{\text{exc}(0 \rightarrow 1)} & -(k_A^{1 \rightarrow 0} + k_A^{\text{exc}(1 \rightarrow 2)}) & k_A^{2 \rightarrow 1} \\ 0 & k_A^{\text{exc}(1 \rightarrow 2)} & k_A^{\text{exc}(1 \rightarrow 2)} \\ 1 & 1 & 1 \end{pmatrix} \times \begin{pmatrix} N^{(0)} \\ N^{(1)} \\ N^{(2)} \end{pmatrix} = \begin{pmatrix} 0 \\ 0 \\ 0 \\ N_{\text{tot}} \end{pmatrix} \quad (\text{A4-3})$$

The mathematical solution of eq. A4-3 requires symmetrization with the help of the transpose matrix  ${}^T\mathbf{M}'$ , followed by inversion to give

$$\begin{pmatrix} N^{(0)} \\ N^{(1)} \\ N^{(2)} \end{pmatrix} = ({}^T\mathbf{M}' \times \mathbf{M}')^{-1} \times {}^T\mathbf{M}' \times \begin{pmatrix} 0 \\ 0 \\ 0 \\ N_{\text{tot}} \end{pmatrix} \quad (\text{A4-4})$$

which is then used for computing normalized steady-state population densities produced by continuous-wave irradiation. The same strategy is used for the molecular systems characterized by their kinetic matrices  $\mathbf{M}$  gathered in Figures S17 and S18.

**Table S1** Elemental analyses for  $[\text{MLn}(\text{L1})_3](\text{CF}_3\text{SO}_3)_6 \cdot m\text{C}_2\text{H}_5\text{CN} \cdot n\text{H}_2\text{O}$  and  $[\text{MLnM}(\text{L2})_3](\text{CF}_3\text{SO}_3)_9 \cdot m\text{C}_2\text{H}_5\text{CN} \cdot n\text{H}_2\text{O}$  complexes (M = Ga, Cr and Ln = Y, Ho, Er, Tm).

Compound	<i>MM</i> / g·mol <sup>-1</sup>	%C found	%H found	%N found	%C Calcd	%H Calcd	%N Calcd
$[\text{GaEr}(\text{L1})_3](\text{CF}_3\text{SO}_3)_6$ <i>m</i> = 1.6 and <i>n</i> = 2.5	2988.80	46.65	3.71	11.67	46.63	3.66	11.72
$[\text{GaY}(\text{L1})_3](\text{CF}_3\text{SO}_3)_6$ <i>m</i> = 2.1 and <i>n</i> = 7.7	3030.39	47.53	3.75	11.48	47.50	3.67	11.54
$[\text{CrEr}(\text{L1})_3](\text{CF}_3\text{SO}_3)_6$ <i>m</i> = 1.0 and <i>n</i> = 5.5	2989.35	46.99	3.61	11.66	46.97	3.57	11.70
$[\text{CrY}(\text{L1})_3](\text{CF}_3\text{SO}_3)_6$ <i>m</i> = 1.8 and <i>n</i> = 4.7	2944.10	48.84	4.05	12.01	48.73	3.72	12.28
$[\text{GaErGa}(\text{L2})_3](\text{CF}_3\text{SO}_3)_9$ <i>m</i> = 2.8 and <i>n</i> = 8.5	4384.12	46.65	3.68	11.42	46.65	3.68	11.42
$[\text{GaYGa}(\text{L2})_3](\text{CF}_3\text{SO}_3)_9$ <i>m</i> = 2.9 and <i>n</i> = 6.2	4268.46	48.03	3.80	11.66	47.99	3.67	11.76
$[\text{CrErCr}(\text{L2})_3](\text{CF}_3\text{SO}_3)_9$ <i>m</i> = 2.8 and <i>n</i> = 4.9	4283.26	47.76	3.62	11.67	47.75	3.60	11.69
$[\text{CrYCr}(\text{L2})_3](\text{CF}_3\text{SO}_3)_9$ <i>m</i> = 4.7 and <i>n</i> = 8.6	4379.03	48.31	3.90	12.07	48.31	3.90	12.06
$[\text{CrHoCr}(\text{L2})_3](\text{CF}_3\text{SO}_3)_9$ <i>m</i> = 0 and <i>n</i> = 9.8	4215.92	46.26	3.74	10.62	46.15	3.55	10.96
$[\text{CrTmCr}(\text{L2})_3](\text{CF}_3\text{SO}_3)_9$ <i>m</i> = 4.8 and <i>n</i> = 9.3	4476.42	47.29	3.76	11.93	47.33	3.86	11.84

**Table S2** Molecular peaks and their triflate adducts observed by ESI-MS (soft positive mode) for  $[\text{MLn}(\text{L1})_3](\text{CF}_3\text{SO}_3)_6 \cdot m\text{CH}_3\text{CH}_2\text{CN} \cdot n\text{H}_2\text{O}$  (Ln = Y, Er) in acetonitrile (total ligand concentration:  $3\text{-}5 \cdot 10^{-4}$  M).

Cationic species	Ln = Y	Ln = Er
	<i>m/z</i>	<i>m/z</i>
$[\text{GaLn}(\text{L1})_3(\text{CF}_3\text{SO}_3)_5]^+$	-	2706.9
$[\text{GaLn}(\text{L1})_3(\text{CF}_3\text{SO}_3)_4]^{2+}$	1237.9	-
$[\text{GaLn}(\text{L1})_3(\text{CF}_3\text{SO}_3)_3]^{3+}$	-	1278
$[\text{CrLn}(\text{L1})_3(\text{CF}_3\text{SO}_3)_5]^+$	2609	2687.4
$[\text{CrLn}(\text{L1})_3(\text{CF}_3\text{SO}_3)_4]^{2+}$	1230	1268.6
$[\text{CrLn}(\text{L1})_3(\text{CF}_3\text{SO}_3)_3]^{3+}$	-	559.7

**Table S3** Molecular peaks and their triflate adducts observed by ESI-MS (soft positive mode) for  $[\text{MLnM}(\text{L2})_3](\text{CF}_3\text{SO}_3)_9 \cdot m\text{CH}_3\text{CH}_2\text{CN} \cdot n\text{H}_2\text{O}$  (Ln = Y, Er, Tm) in acetonitrile (total ligand concentration:  $3\text{-}5 \cdot 10^{-4}$  M).

Cationic species	Ln = Y	Ln = Er	Ln = Tm
	<i>m/z</i>	<i>m/z</i>	<i>m/z</i>
$[\text{GaLnGa}(\text{L2})_3(\text{CF}_3\text{SO}_3)_7]^{2+}$	1850	1889.8	<sup>a</sup>
$[\text{GaLnGa}(\text{L2})_3(\text{CF}_3\text{SO}_3)_6]^{3+}$	1187	1210	<sup>a</sup>
$[\text{GaLnGa}(\text{L2})_3(\text{CF}_3\text{SO}_3)_5]^{4+}$	-	870	<sup>a</sup>
$[\text{GaLnGa}(\text{L2})_3(\text{CF}_3\text{SO}_3)]^{8+}$	351	-	<sup>a</sup>
$[\text{CrLnCr}(\text{L2})_3(\text{CF}_3\text{SO}_3)_7]^{2+}$	1832.8	1872.6	1872.3
$[\text{CrLnCr}(\text{L2})_3(\text{CF}_3\text{SO}_3)_6]^{3+}$	1172.3	1198.3	1198.8
$[\text{CrLnCr}(\text{L2})_3(\text{CF}_3\text{SO}_3)_5]^{4+}$	842	862	862
$[\text{CrLnCr}(\text{L2})_3(\text{CF}_3\text{SO}_3)_4]^{5+}$	644	-	-
$[\text{CrLnCr}(\text{L2})_3(\text{CF}_3\text{SO}_3)_3]^{6+}$	-	525	-
$[\text{CrLnCr}(\text{L2})_3(\text{CF}_3\text{SO}_3)_2]^{7+}$	417	429	-
$[\text{CrLnCr}(\text{L2})_3(\text{CF}_3\text{SO}_3)]^{8+}$	-	356	-

<sup>a</sup> Complex not isolated.

**Table S4.** Summary of crystal data, intensity measurements and structure refinements for [GaErGa(L2)<sub>3</sub>](CF<sub>3</sub>SO<sub>3</sub>)<sub>9</sub>(CH<sub>3</sub>CN)<sub>35.5</sub> (**16**)

	[Ga <sub>2</sub> Er(L2) <sub>3</sub> ](CF <sub>3</sub> SO <sub>3</sub> ) <sub>9</sub>	[Cr <sub>2</sub> Yb(L2) <sub>3</sub> ](CF <sub>3</sub> SO <sub>3</sub> ) <sub>9</sub> <sup>a</sup>	[Cr <sub>2</sub> Eu(L2) <sub>3</sub> ](CF <sub>3</sub> SO <sub>3</sub> ) <sub>9</sub> <sup>a</sup>
Empirical formula	C <sub>484</sub> H <sub>471</sub> Er <sub>2</sub> F <sub>54</sub> Ga <sub>4</sub> N <sub>137</sub> O <sub>54</sub> S <sub>18</sub>	C <sub>414</sub> H <sub>408</sub> Cr <sub>4</sub> Yb <sub>2</sub> F <sub>54</sub> N <sub>96</sub> O <sub>54</sub> S <sub>18</sub>	C <sub>414</sub> H <sub>408</sub> Cr <sub>4</sub> Eu <sub>2</sub> F <sub>54</sub> N <sub>96</sub> O <sub>54</sub> S <sub>18</sub>
Formula weight	11287.46	9749.41	9707.26
Temperature	150(2)K	100(2)K	100(2)K
Wavelength	1.54184 Å	0.70000 Å	0.70000 Å
Crystal System, Space group	Monoclinic, <i>P</i> 2 <sub>1</sub> / <i>c</i>	Monoclinic, <i>P</i> 2 <sub>1</sub> / <i>c</i>	Monoclinic, <i>P</i> 2 <sub>1</sub> / <i>c</i>
Unit cell dimensions	<i>a</i> = 29.3602(5) Å <i>b</i> = 61.334(2) Å <i>c</i> = 26.7917(3) Å <i>α</i> = 90° <i>β</i> = 98.9550(10)° <i>γ</i> = 90°	<i>a</i> = 29.5080(10) Å <i>b</i> = 61.8320(2) Å <i>c</i> = 26.831(1) Å <i>α</i> = 90° <i>β</i> = 99.40(2)° <i>γ</i> = 90°	<i>a</i> = 29.3890(4) Å <i>b</i> = 61.0950(10) Å <i>c</i> = 26.6462(3) Å <i>α</i> = 90° <i>β</i> = 99.375(2)° <i>γ</i> = 90°
Volume in Å <sup>3</sup>	47657.8(18)	48294(29)	47204.8(11)
Z, Calculated density	4, 1.573 Mg/m <sup>3</sup>	4, 1.34 Mg/m <sup>3</sup>	4, 1.37 Mg/m <sup>3</sup>
Absorption coefficient	2.539 mm <sup>-1</sup>		
<i>F</i> (000)	23200		
Theta range for data collection	2.64 to 61.71°	3.25 to 18.85	1.48 to 21.62
Limiting indices	-33 ≤ <i>h</i> ≤ 33, -65 ≤ <i>k</i> ≤ 68, -28 ≤ <i>l</i> ≤ 30		
Reflections collected / unique	147871 / 70625 [ <i>R</i> (int) = 0.0892]		
Completeness to theta	94.9 %		
Data / restraints / parameters	70625 / 257 / 3940		
Goodness-of-fit on <i>F</i> <sup>2</sup>	1.444		
Final <i>R</i> indices [ <i>I</i> > 2σ( <i>I</i> )]	<i>R</i> <sub>1</sub> = 0.1300, <i>ωR</i> <sub>2</sub> = 0.2972		
<i>R</i> indices (all data)	<i>R</i> <sub>1</sub> = 0.1816, <i>ωR</i> <sub>2</sub> = 0.3162		
Largest diff. peak and hole	3.045 and -1.427e·Å <sup>-3</sup>		

<sup>a</sup> Taken from reference 10 for comparison purpose.

**Table S5** Summary of crystal data, intensity measurements and structure refinements for  
 $[\text{CrEr}(\text{L1})_3](\text{CF}_3\text{SO}_3)_6(\text{C}_3\text{H}_5\text{N})_{26}$  (**17**)

Empirical formula	C192 H220 Cr Er F18 N50 O18 S6	
Chemical formula moiety	'C108 H90 Cr Er N24, 6(C F3 S O3), 26(C3 H5 N)'	
Formula weight	4269.80	
Temperature	100(2) K	
Wavelength	0.8231 Å	
Crystal system	Trigonal	
Space group	P -3 1 m	
Unit cell dimensions	$a = 26.4289(3)$ Å	$\alpha = 90^\circ$ .
	$b = 26.4289(3)$ Å	$\beta = 90^\circ$ .
	$c = 36.9113(4)$ Å	$\gamma = 120^\circ$ .
Volume	22328.0(5) Å <sup>3</sup>	
Z	4	
Density (calculated)	1.270 Mg/m <sup>3</sup>	
Absorption coefficient	0.826 mm <sup>-1</sup>	
F(000)	8864	
Crystal size	0.353 x 0.236 x 0.072 mm <sup>3</sup>	
Theta range for data collection	1.64 to 25.53°.	
Index ranges	-26 ≤ $h$ ≤ 27, -27 ≤ $k$ ≤ 27, -38 ≤ $l$ ≤ 38	
Reflections collected	53729	
Independent reflections	8666 [ $R(\text{int}) = 0.0656$ ]	
Completeness to theta = 25.53°	92.1 %	
Absorption correction	Semi-empirical from equivalents	
Max. and min. transmission	1.00000 and 0.81691	
Refinement method	Full-matrix least-squares on $F^2$	
Data / restraints / parameters	8666 / 0 / 407	
Goodness-of-fit on $F^2$	0.974	
Final R indices [ $I > 2\sigma(I)$ ]	$R1 = 0.0445$ , $wR2 = 0.1195$	
R indices (all data)	$R1 = 0.0620$ , $wR2 = 0.1248$	
Largest diff. peak and hole	0.307 and -0.243 e·Å <sup>-3</sup>	

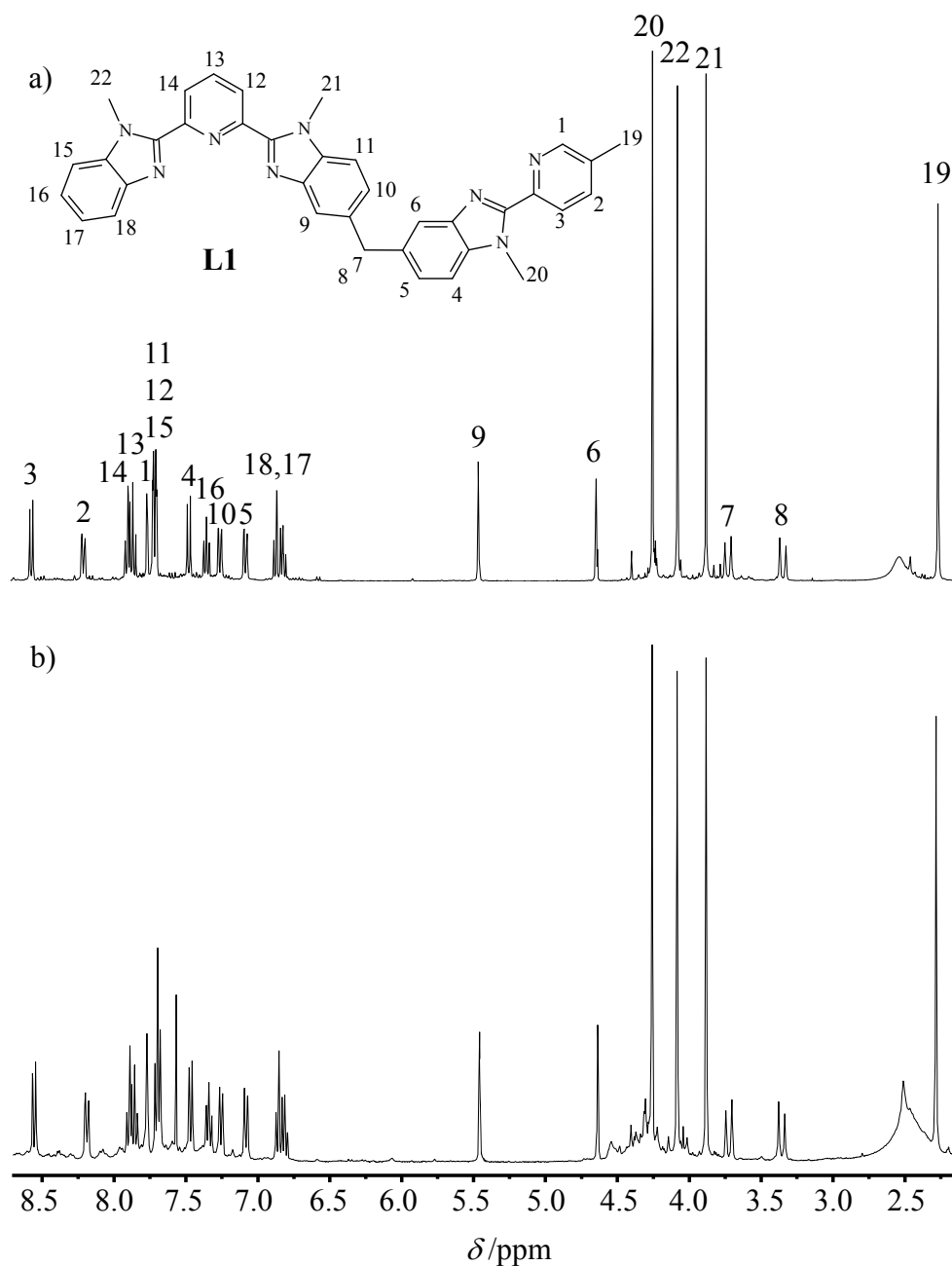


**Figure S1**  $^1\text{H}$  NMR spectra with assignment for a) crystals of  $[\text{GaY}(\text{L1})_3](\text{CF}_3\text{SO}_3)_6$  dissolved in  $\text{CD}_3\text{CN}$  and b) mixtures of **L1** (3.0 eq.),  $\text{Ga}(\text{CF}_3\text{SO}_3)_3$  (1.0 eq.) and  $\text{Y}(\text{CF}_3\text{SO}_3)_3$  (1.0 eq.) after 24 h at  $50^\circ\text{C}$  in  $\text{CD}_3\text{CN}$ .

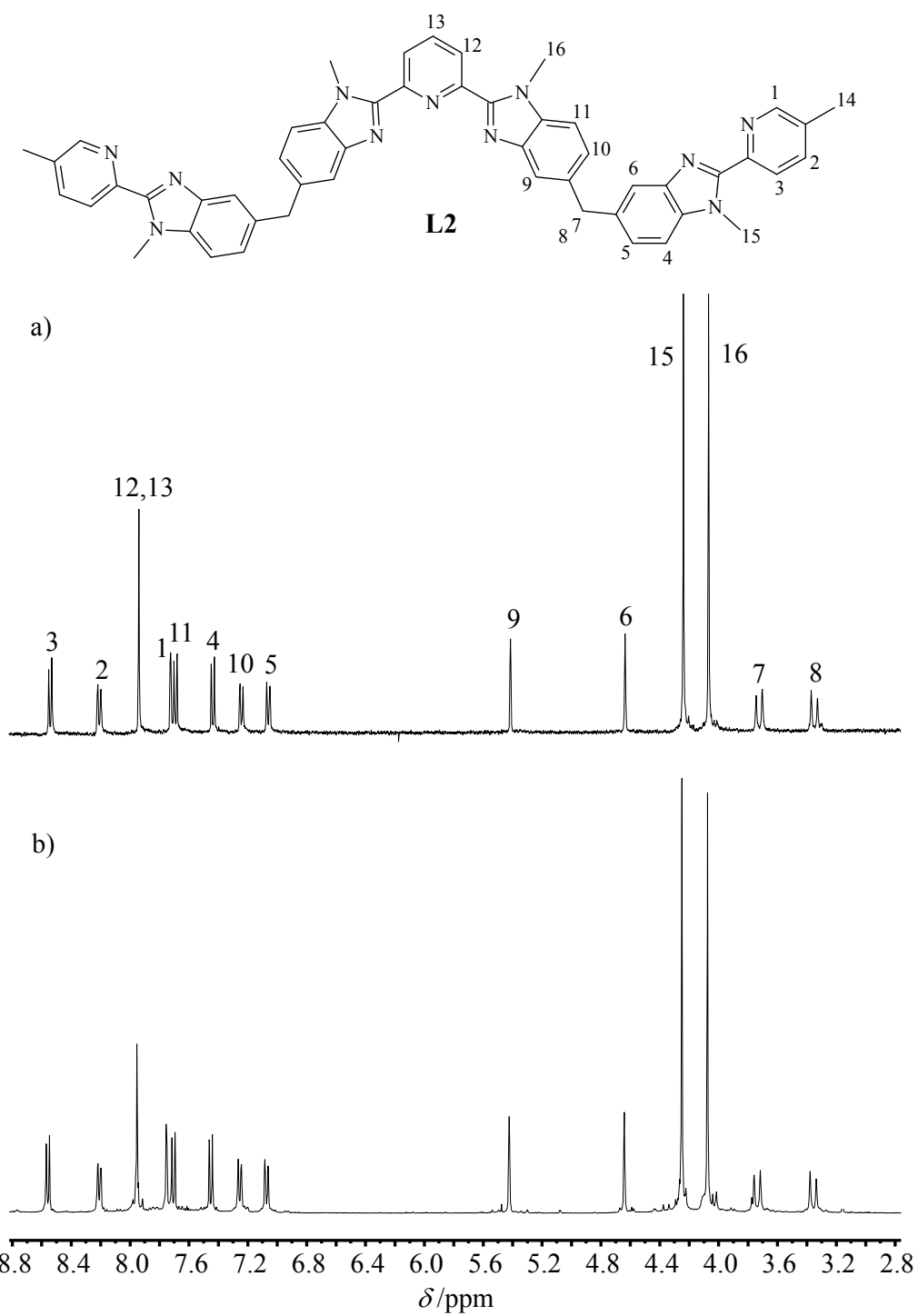


**Figure S2**  $^1\text{H}$  NMR spectra with assignment for a) crystals of  $[\text{GaYGa}(\text{L2})_3](\text{CF}_3\text{SO}_3)_9$  dissolved in  $\text{CD}_3\text{CN}$  and b) mixtures of **L2** (3.0 eq.),  $\text{Ga}(\text{CF}_3\text{SO}_3)_3$  (2.0 eq.) and  $\text{Y}(\text{CF}_3\text{SO}_3)_3$  (1.0 eq.) after 50 h at  $55^\circ\text{C}$  in  $\text{CD}_3\text{CN}$ .

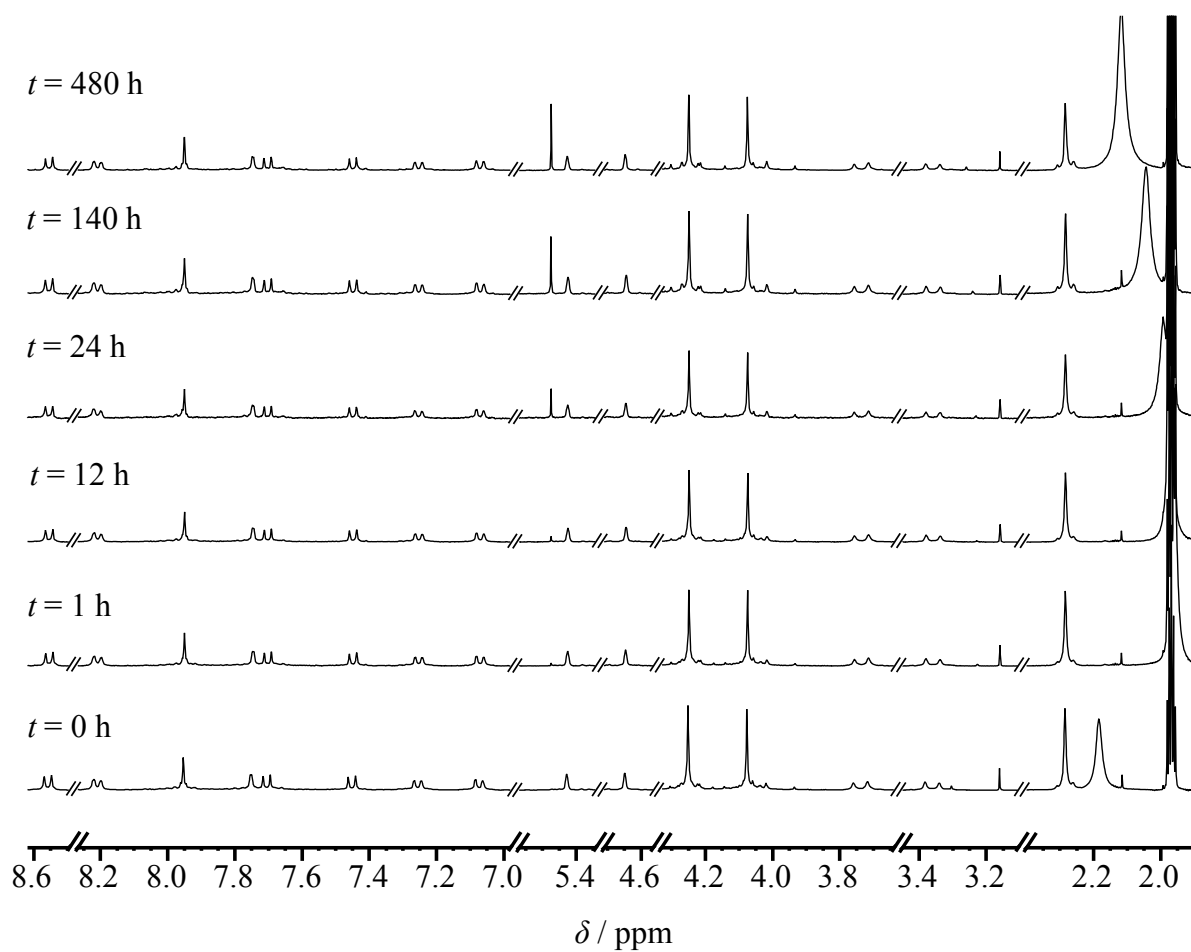


**Figure S3** Reaction of  $[\text{GaYGa}(\text{L}2)_3](\text{CF}_3\text{SO}_3)_9$  (1.0 eq) with  $\text{Eu}(\text{CF}_3\text{SO}_3)_3$  (1.0 eq) monitored by  $^1\text{H}$  NMR in  $\text{CD}_3\text{CN}$  at 293 K for 20 days.

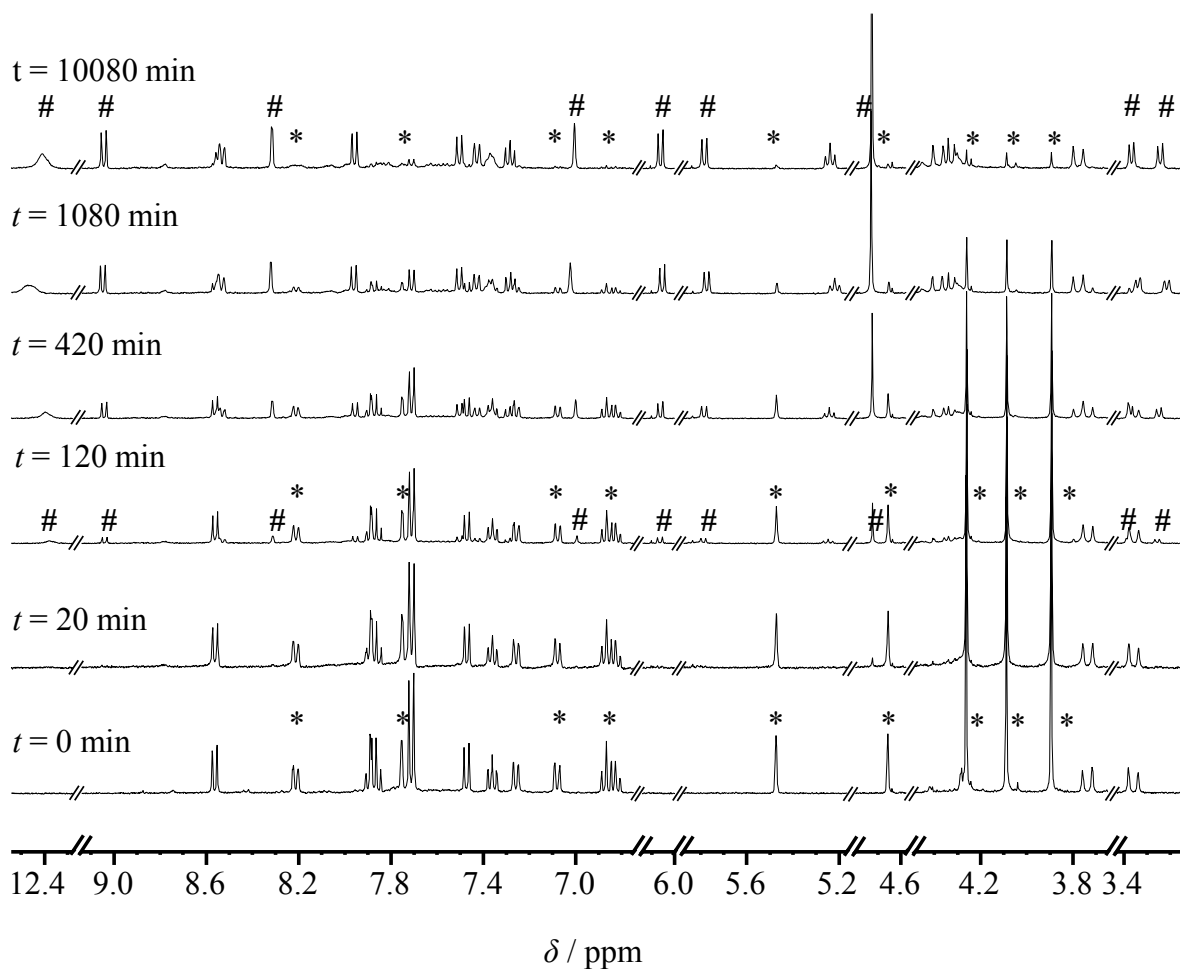


**Figure S4** Reaction of  $[\text{GaY}(\text{L1})_3](\text{CF}_3\text{SO}_3)_6$  (1.0 eq) with  $\text{Eu}(\text{CF}_3\text{SO}_3)_3$  (1.0 eq) monitored by  $^1\text{H}$  NMR in  $\text{CD}_3\text{CN}$  at 293 K for 7 days (\* correspond to the signals integrated for quantifying  $[\text{GaY}(\text{L1})_3]^{6+}$ , while # stand for those used for  $[\text{GaEu}(\text{L1})_3]^{6+}$ ).

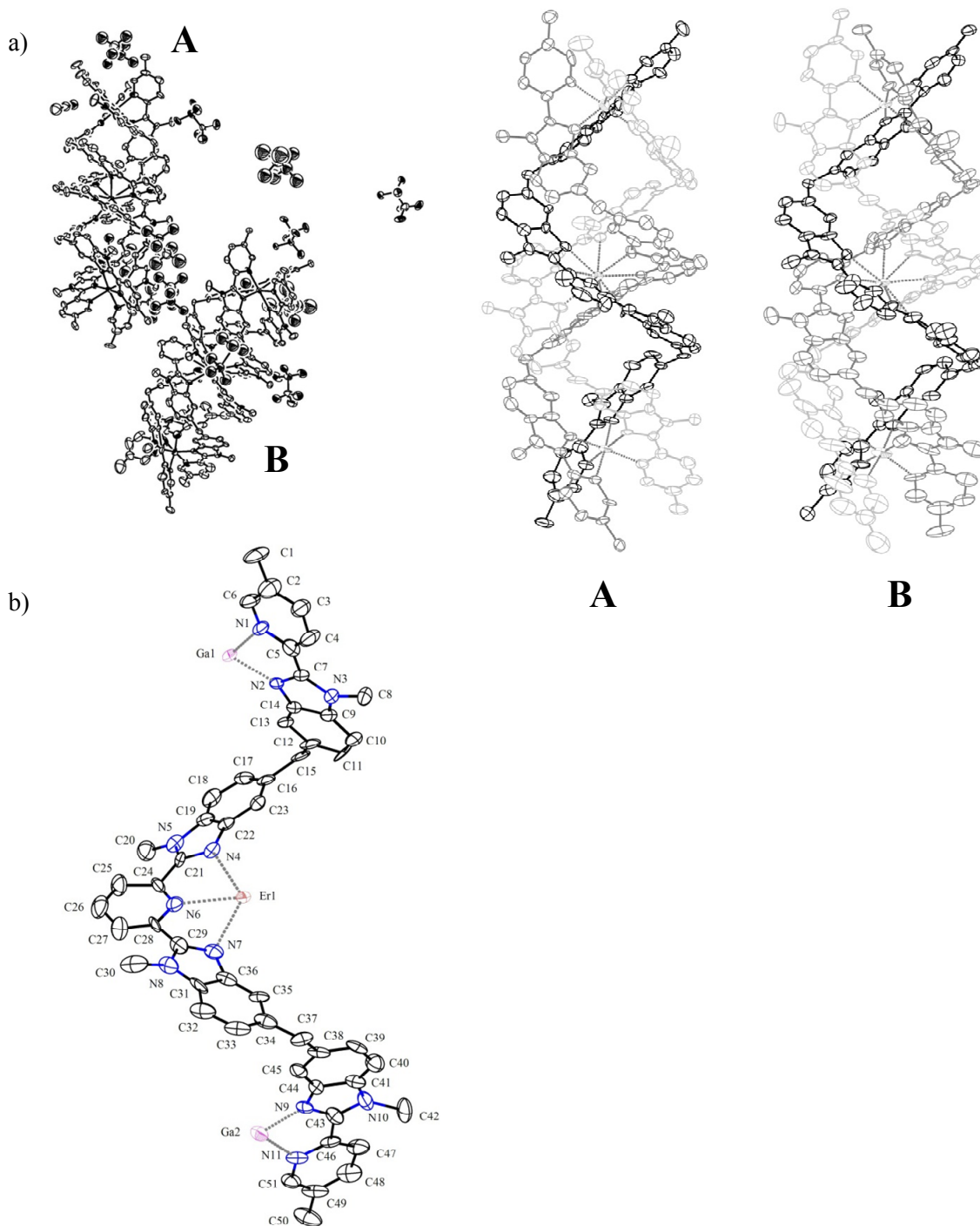


**Figure S5** a) ORTEP view of the molecular structures of the two triple-helical  $[\text{GaErGa}(\text{L}2)_3]^{9+}$  cations A and B along their pseudo-threefold axes in the asymmetric unit of  $[\text{GaErGa}(\text{L}2)_3](\text{CF}_3\text{SO}_3)_9(\text{C}_2\text{H}_5\text{N})_{35.5}$ . b) Numbering scheme of a ligand strand. Ellipsoids are represented at the 30% probability level. Hydrogen atoms are omitted for clarity.

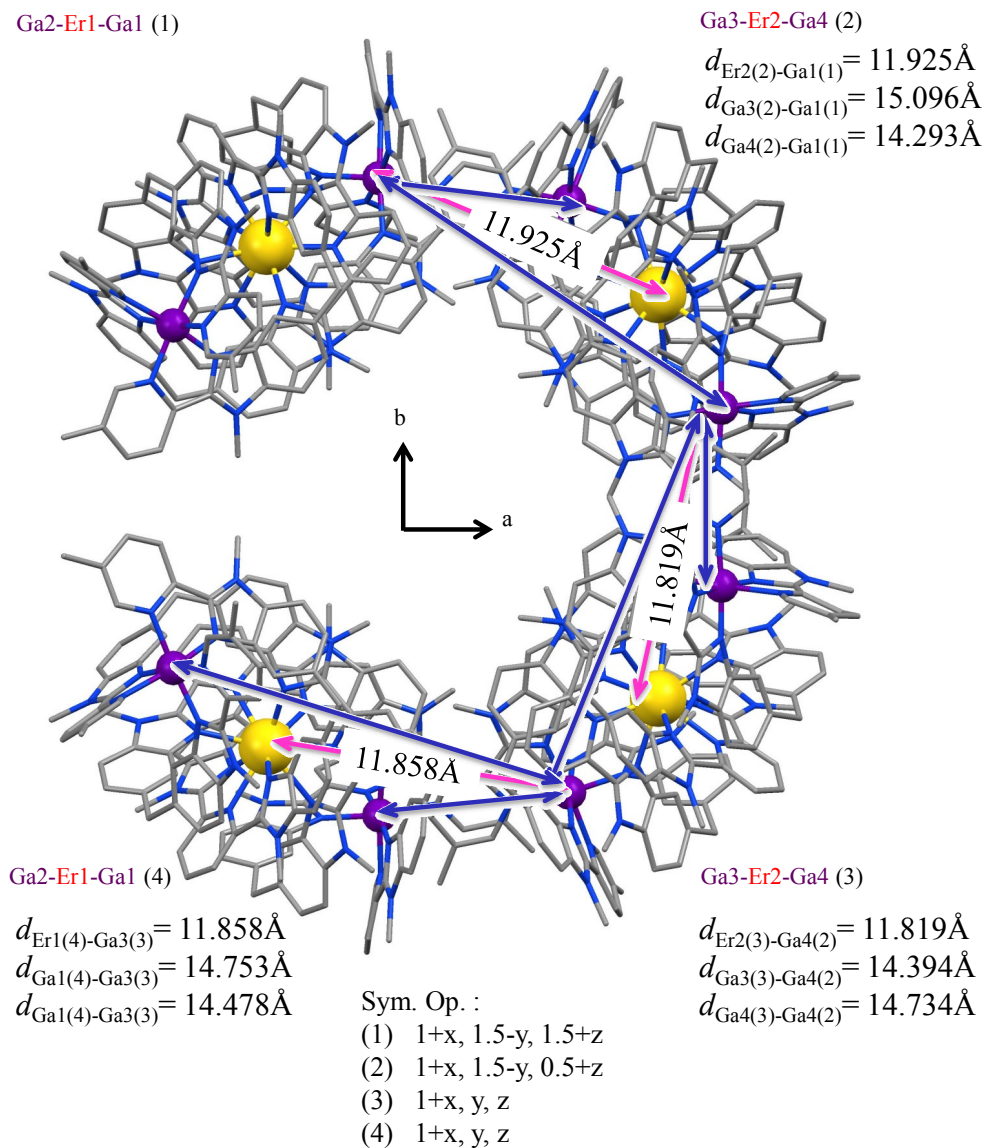


**Figure S6** View of the crystal packing along the  $\bar{c}$  direction in the crystal structure of  $[\text{GaErGa}(\mathbf{L2})_3](\text{CF}_3\text{SO}_3)_9(\text{C}_2\text{H}_3\text{N})_{35.5}$  showing the shortest intermolecular intermetallic distances.

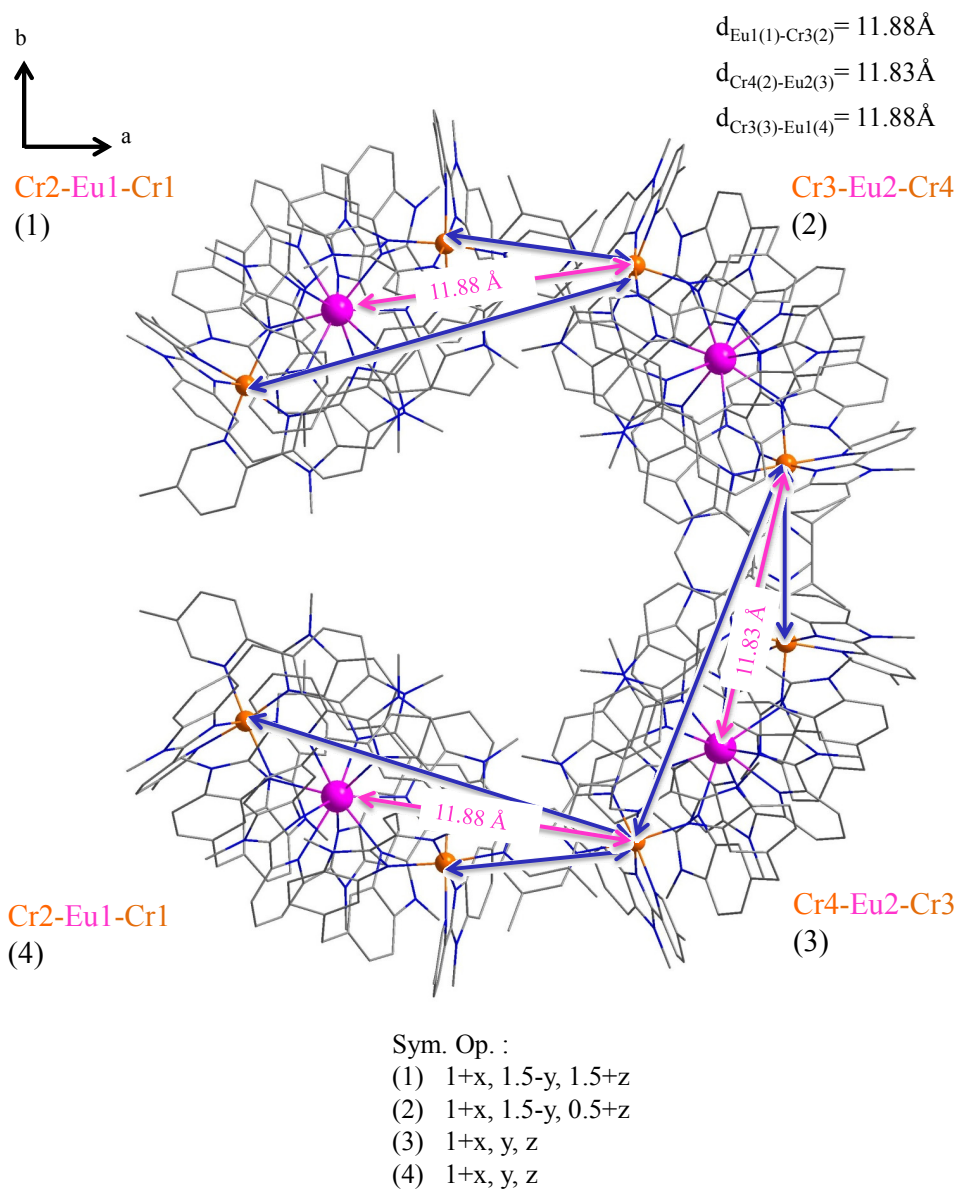


**Figure S7** View of the crystal packing along the  $\bar{c}$  direction in the crystal structure of  $[\text{CrEuCr}(\text{L2})_3](\text{CF}_3\text{SO}_3)_9(\text{C}_3\text{H}_5\text{N})_{15}$  showing the shortest intermolecular intermetallic distances.<sup>10</sup>

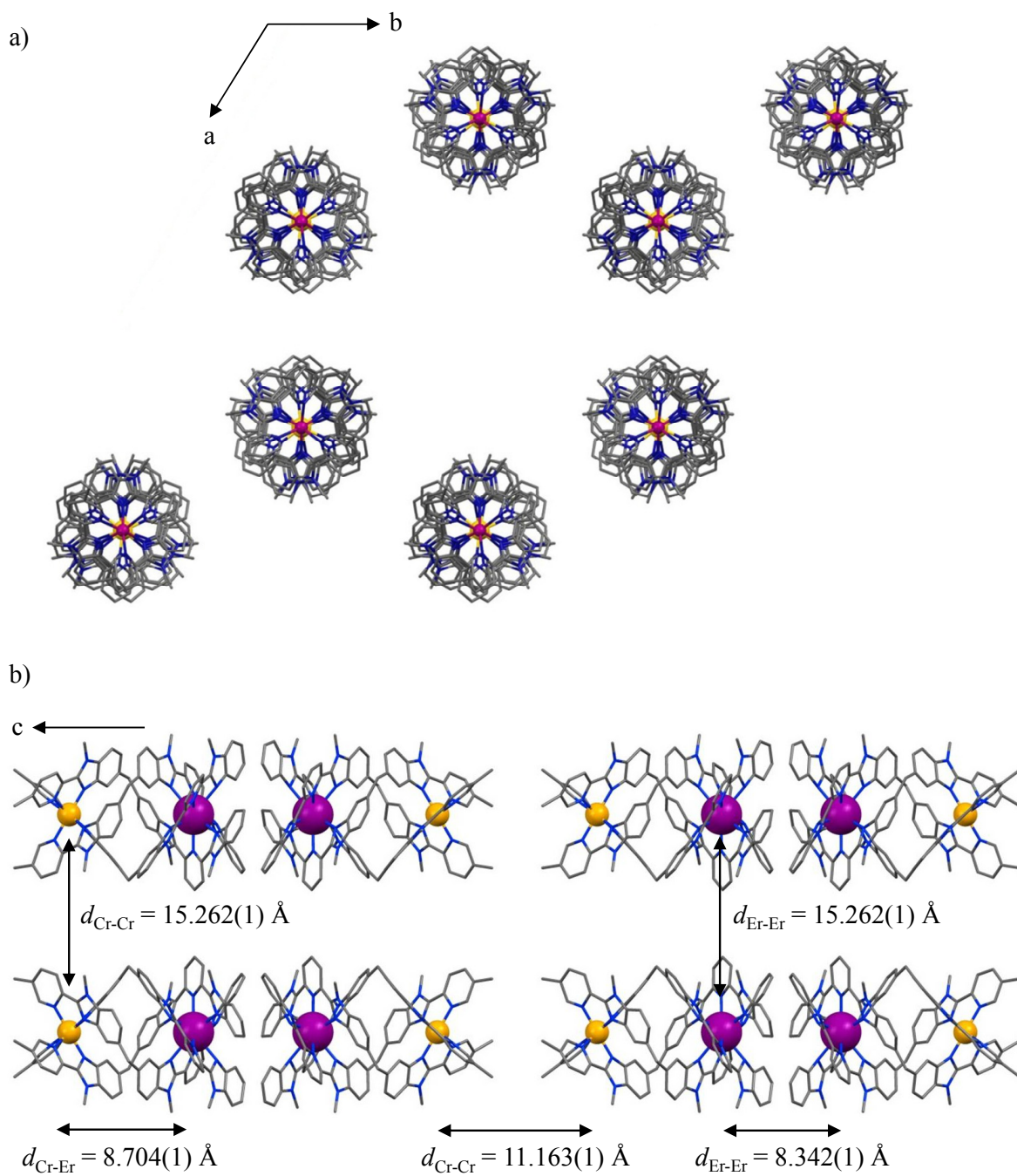


**Figure S8** View of the crystal packing (a) along the  $\bar{c}$  direction and (b) along the [110] direction in the crystal structure of  $[\text{CrEr}(\text{L1})_3](\text{CF}_3\text{SO}_3)_6(\text{C}_3\text{H}_5\text{N})_{26}$  showing the shortest intermetallic distances.

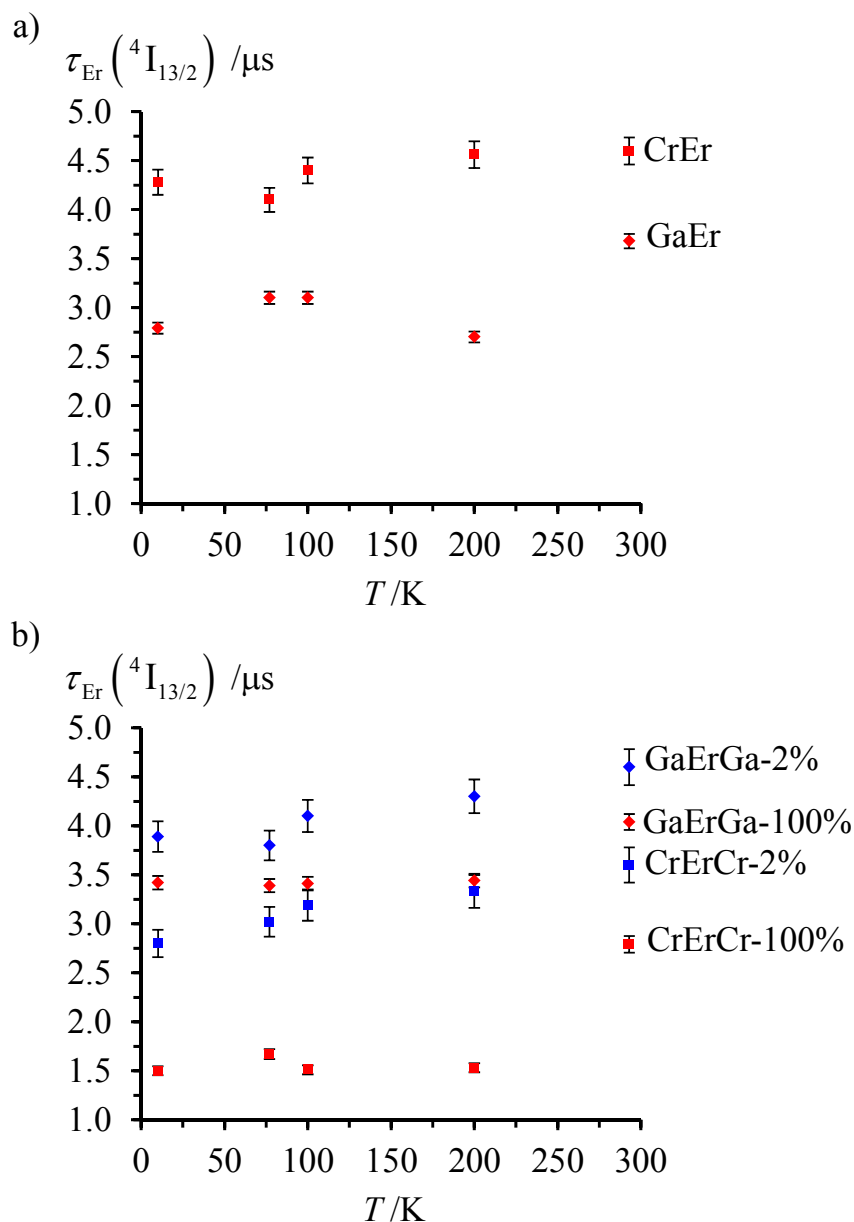


**Figure S9** Solid-state mono-exponential characteristic  $\text{Er}(^4\text{I}_{13/2})$  lifetimes measured for (a)  $[\text{MEr}(\text{L1})_3](\text{CF}_3\text{SO}_3)_6$  ( $M = \text{Ga}$  as diamonds;  $M = \text{Cr}$  as squares,  $\tilde{\nu}_{\text{exc}} = 28169 \text{ cm}^{-1}$  or  $\lambda_{\text{exc}} = 355 \text{ nm}$ ) and (b)  $[\text{MErM}(\text{L2})_3](\text{CF}_3\text{SO}_3)_9$  ( $M = \text{Ga}$  as diamond;  $M = \text{Cr}$  with squares,  $\tilde{\nu}_{\text{exc}} = 28169 \text{ cm}^{-1}$  or  $\lambda_{\text{exc}} = 355 \text{ nm}$ ) at various temperatures. Color code: red markers refer to pure compound, while blue markers are used for 2%  $[\text{MErM}(\text{L2})_3](\text{CF}_3\text{SO}_3)_9$  dispersed in  $[\text{GaYGa}(\text{L2})_3](\text{CF}_3\text{SO}_3)_9$ . The numerical values with esds can be found in ref. 11.

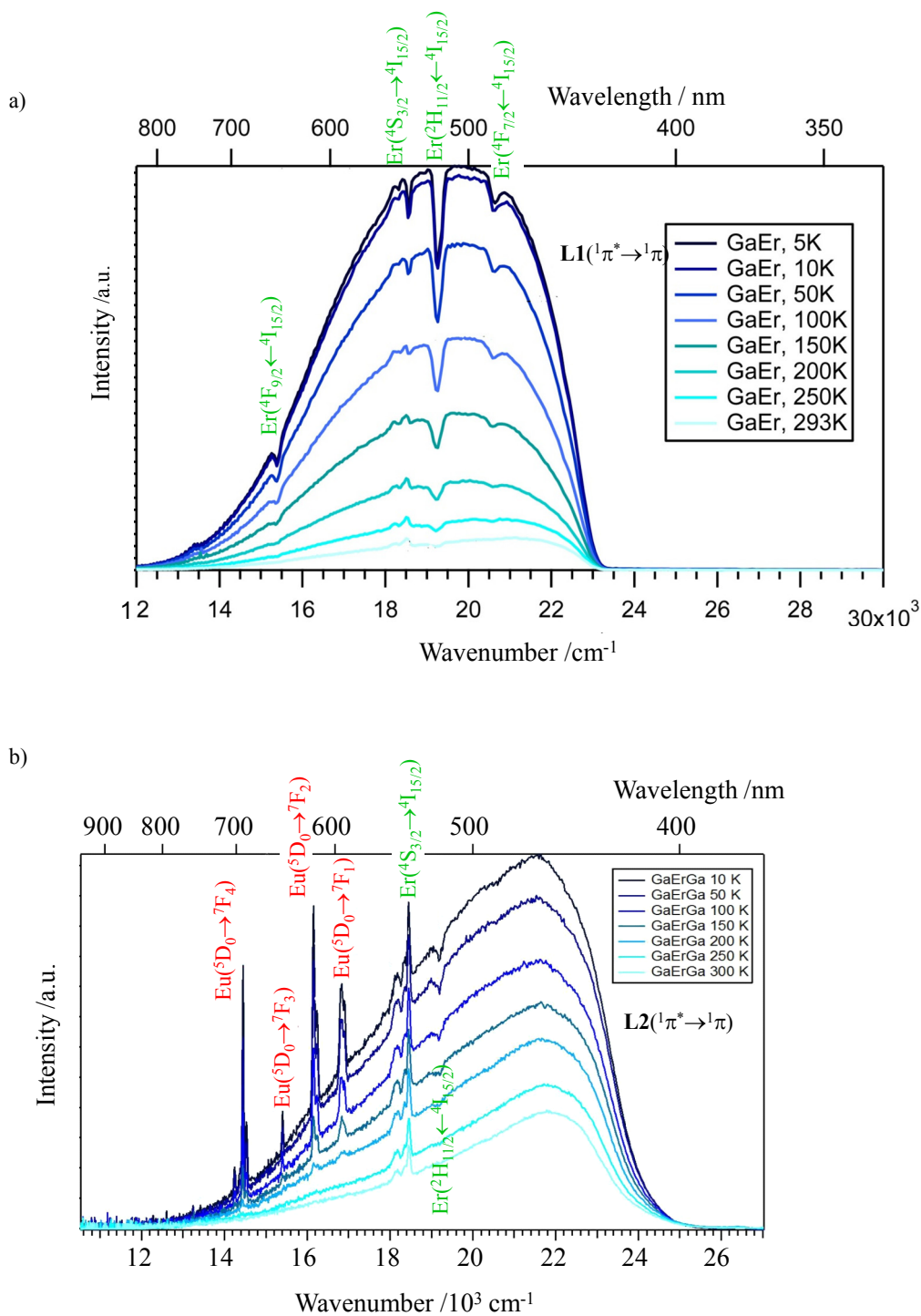


**Figure S10** Solid-state emission spectra recorded for (a) [GaEr(L1)<sub>3</sub>](CF<sub>3</sub>SO<sub>3</sub>)<sub>6</sub> ( $\tilde{\nu}_{\text{exc}} = 24691 \text{ cm}^{-1}$  or  $\lambda_{\text{exc}} = 405 \text{ nm}$ , cutoff at 435 nm) and (b) [GaErGa(L2)<sub>3</sub>](CF<sub>3</sub>SO<sub>3</sub>)<sub>9</sub> ( $\tilde{\nu}_{\text{exc}} = 28169 \text{ cm}^{-1}$  or  $\lambda_{\text{exc}} = 355 \text{ nm}$ ) at various temperatures. Er-centred transitions in green and Eu-centred transition in red.<sup>18</sup> The dips correspond to internal Er-centred re-absorption of ligand-centred emission.<sup>13g</sup>

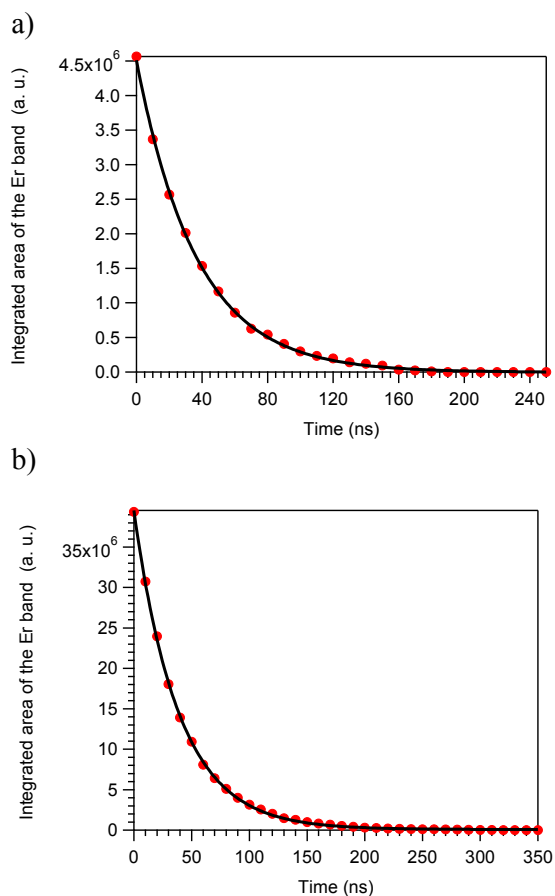


**Figure S11** Luminescence decay traces recorded for the  $\text{Er}(^4\text{S}_{3/2} \rightarrow ^4\text{I}_{15/2})$  transitions in (a)  $[\text{GaEr}(\text{L1})_3](\text{CF}_3\text{SO}_3)_6$  and (b)  $[\text{GaErGa}(\text{L2})_3](\text{CF}_3\text{SO}_3)_9$  at 3K in the solid state ( $\lambda_{\text{exc}} = 355 \text{ nm}$ ,  $\tilde{\nu}_{\text{exc}} = 28169 \text{ cm}^{-1}$  and  $\lambda_{\text{an}} = 541 \text{ nm}$ ,  $\tilde{\nu}_{\text{an}} = 18484 \text{ cm}^{-1}$ ). The dark curves correspond to the best fits mono-exponential fits.

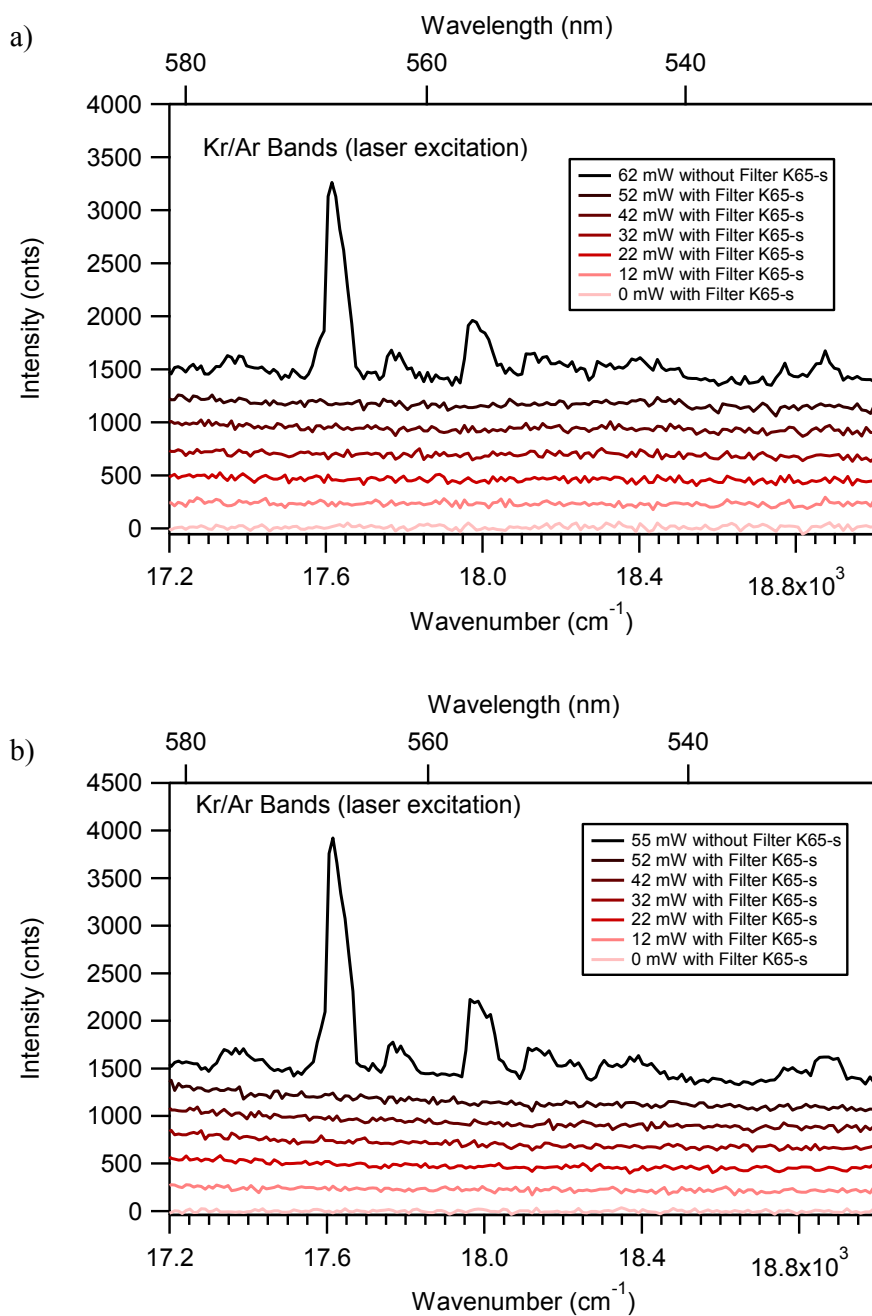


**Figure S12** Attempts to induce one ion ESA upon irradiation of the  $\text{Er}(^4\text{F}_{9/2} \leftarrow ^4\text{I}_{15/2})$  transition in (a)  $[\text{GaEr}(\text{L1})_3](\text{CF}_3\text{SO}_3)_6$  and (b)  $[\text{GaErGa}(\text{L2})_3](\text{CF}_3\text{SO}_3)_9$ , at 5 K (CCD,  $\lambda_{\text{exc}} = 647.1 \text{ nm}$ ,  $\tilde{\nu}_{\text{exc}} = 15454 \text{ cm}^{-1}$ , integration time = 20000 ms, slits aperture = 0.3 mm, filter K-55s (550 nm) + C3C9 for the emission recorded and K-65s (650 nm) for the incident laser beam, incident power = 0-52 mW, the excitation beam was loosely focused on the sample with a 100 mm lens).

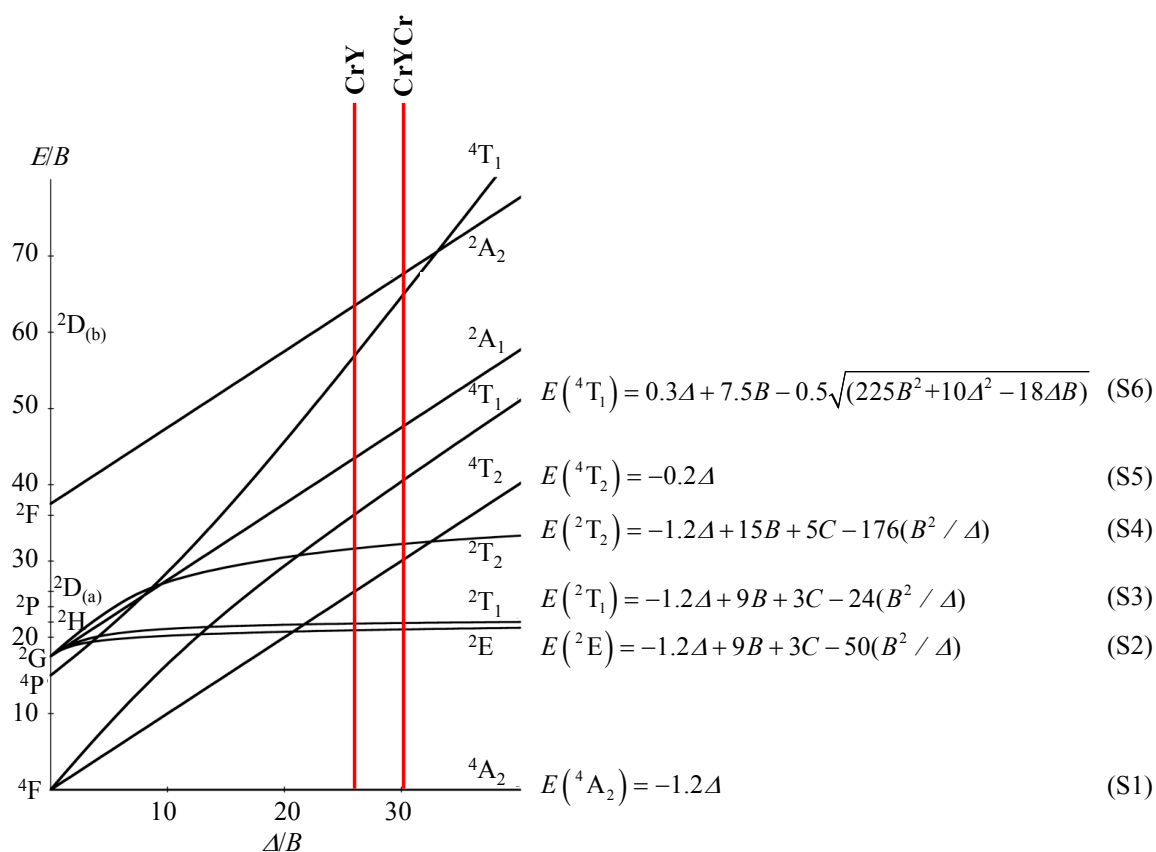


**Figure S13** Energy level diagram (Tanabe-Sugano) for  $d^3$  ions in an octahedral field ( $C = 4.5B$ ). The  $\Delta/B$  ratios found for  $[\text{CrY}(\mathbf{L1})_3](\text{CF}_3\text{SO}_3)_6$  and  $[\text{CrYCr}(\mathbf{L2})_3](\text{CF}_3\text{SO}_3)_9$  are highlighted.<sup>11</sup>

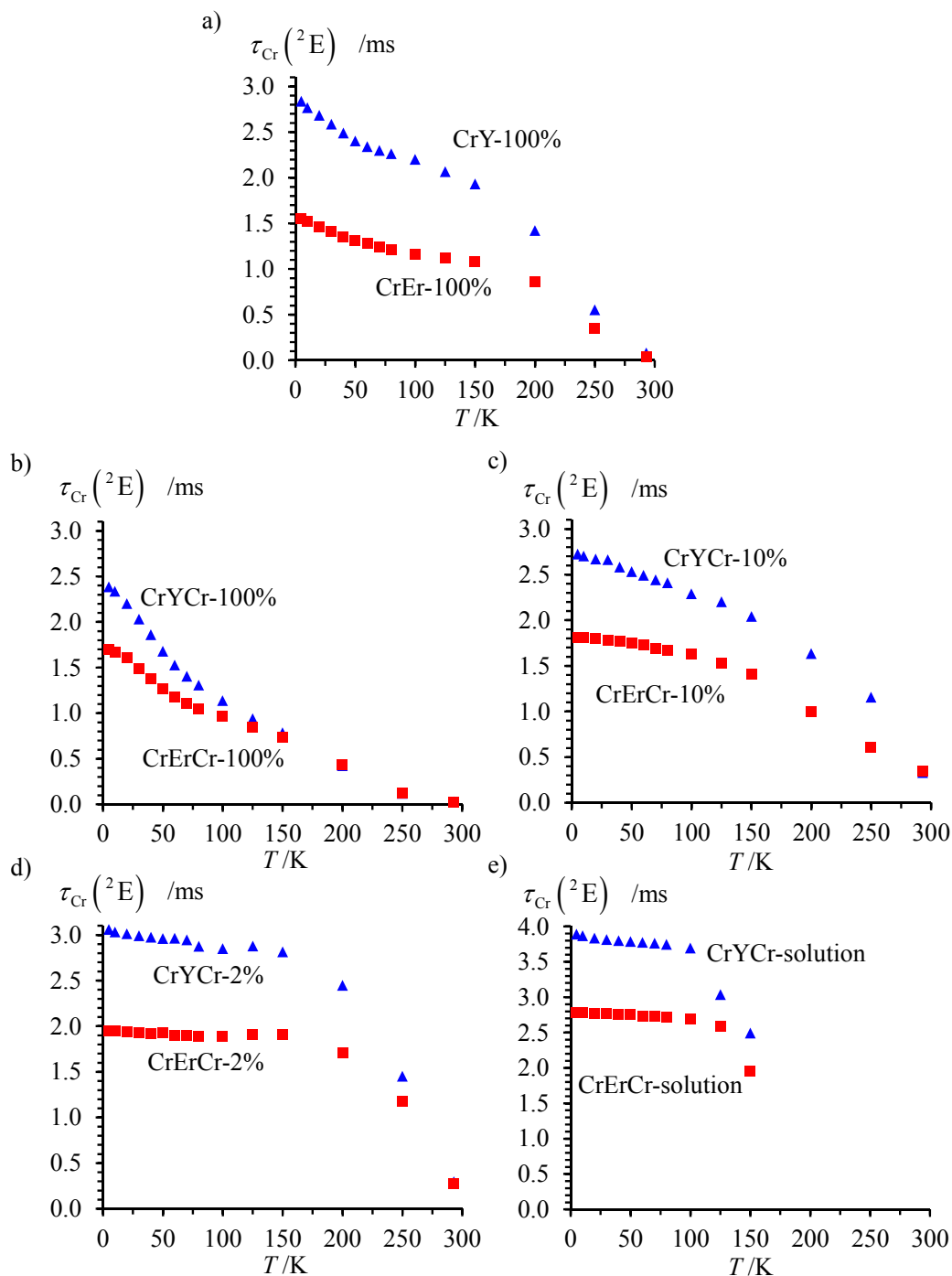


**Figure S14** Characteristic  $\text{Cr}(^2\text{E})$  lifetimes measured for (a)  $[\text{CrLn}(\text{L1})_3](\text{CF}_3\text{SO}_3)_6$  (solid-state 100%), (b)  $[\text{CrLnCr}(\text{L2})_3](\text{CF}_3\text{SO}_3)_9$  (solid state 100%), (c)-(d)  $[\text{CrLnCr}(\text{L2})_3](\text{CF}_3\text{SO}_3)_9$  (solid state x% diluted in  $[\text{GaYGa}(\text{L2})_3](\text{CF}_3\text{SO}_3)_9$ ) and (e)  $[\text{CrLnCr}(\text{L2})_3]^{9+}$  (1 mM in acetonitrile) at various temperatures. Blue triangles correspond to  $\text{Ln} = \text{Y}$  while red squares stand for  $\text{Ln} = \text{Er}$  ( $\tilde{\nu}_{\text{exc}} = 28169 \text{ cm}^{-1}$  or  $\lambda_{\text{exc}} = 355 \text{ nm}$ ).

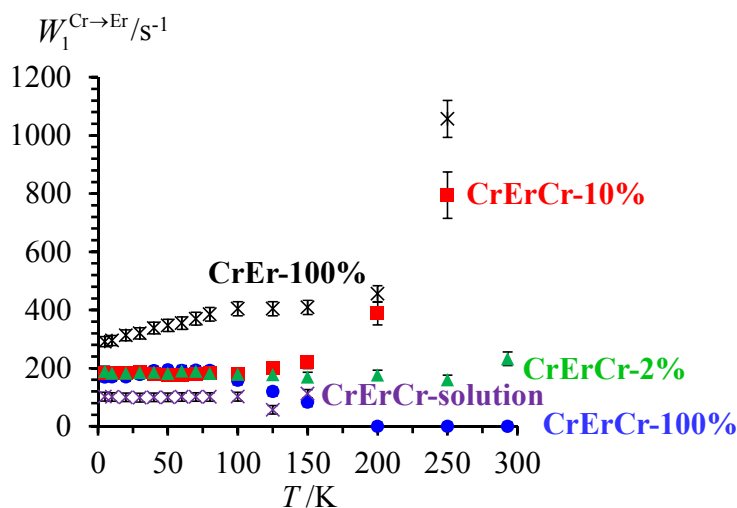


**Figure S15** Rate constants computed with eq. (5) for the  $\text{Cr}({}^2\text{E}) \rightarrow \text{Er}({}^4\text{I}_{9/2})$  energy transfer processes occurring in  $[\text{CrEr}(\text{L1})_3](\text{CF}_3\text{SO}_3)_6$  (solid-state 100%, black crosses) and in  $[\text{CrErCr}(\text{L2})_3](\text{CF}_3\text{SO}_3)_9$  (solid-state 100% = blue disks; solid-state 10% in GaYGa = red squares, solid-state 2% in GaYGa = green triangles, 1 mM in acetonitrile = magenta crosses). Full tables with esds can be found in ref. 11.

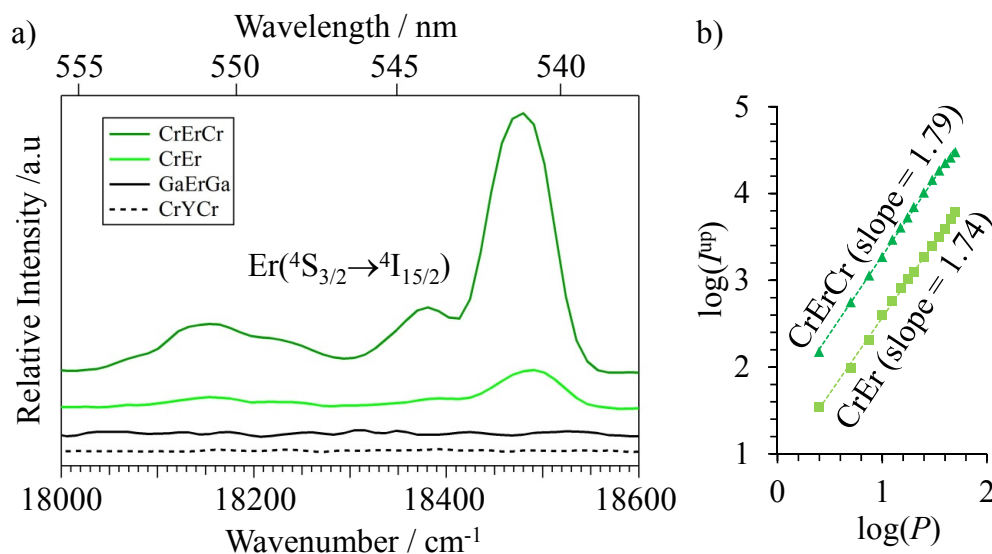
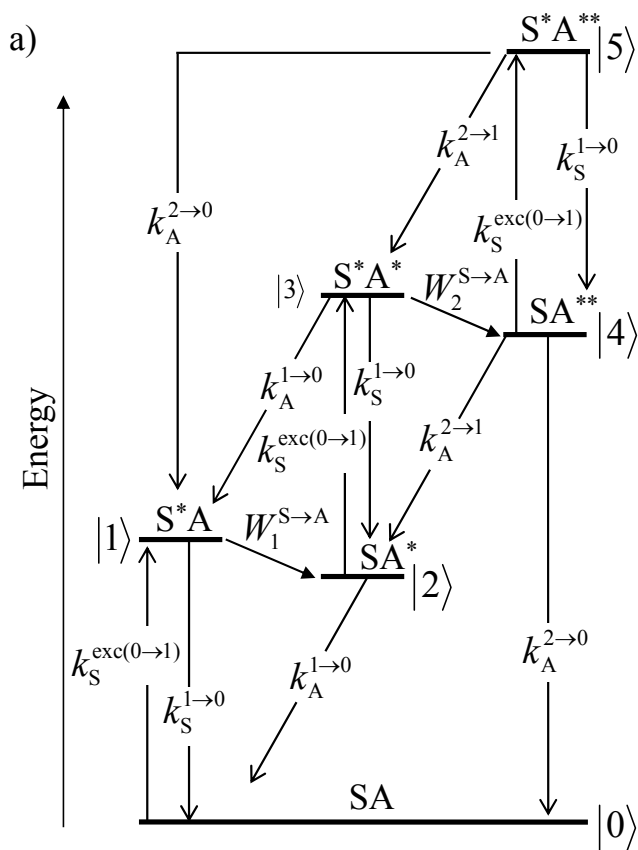


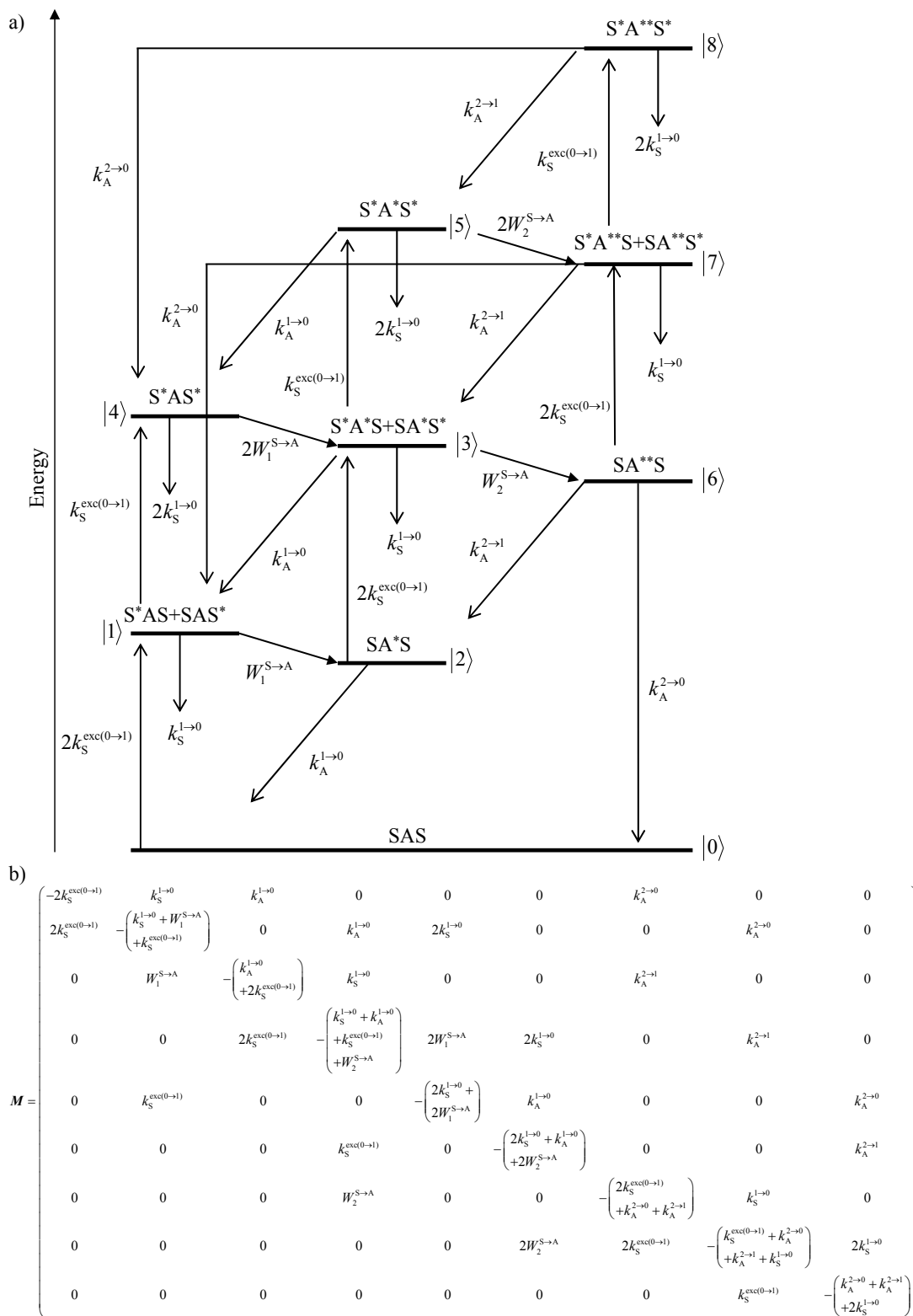
**Figure S16** a) Green upconverted  $\text{Er}({}^4\text{S}_{3/2} \rightarrow {}^4\text{I}_{15/2})$  emission observed for  $[\text{CrEr}(\text{L1})_3](\text{CF}_3\text{SO}_3)_6$  and  $[\text{CrErCr}(\text{L2})_3](\text{CF}_3\text{SO}_3)_9$  in frozen solution (10 mM in acetonitrile:propionitrile (4:1), 31 K,  $\tilde{\nu}_{\text{exc}} = 13986 \text{ cm}^{-1}$  or  $\lambda_{\text{exc}} = 715 \text{ nm}$ ,  $P = 100 \text{ mW}$  loosely focused onto the sample). For direct comparison background spectra recorded under the same conditions for the reference CrYCr and GaErGa systems are included. b) log-log plot of the upconverted emission intensity ( $I^{\text{up}}$ ) with respect to incident pump intensity into the  $\text{Cr}({}^2\text{T}_1 \leftarrow {}^4\text{A}_2)$  transition ( $P$  in mW) for CrEr and CrErCr (symbols = experimental points, lines = linear fits). Adapted from ref. 11.



b)

$$\mathbf{M} = \begin{pmatrix} -k_S^{exc(0\rightarrow1)} & k_S^{1\rightarrow0} & k_A^{1\rightarrow0} & 0 & k_A^{2\rightarrow0} & 0 \\ k_S^{exc(0\rightarrow1)} & -(k_S^{1\rightarrow0} + W_1^{S\rightarrow A}) & 0 & k_A^{1\rightarrow0} & 0 & k_A^{2\rightarrow0} \\ 0 & W_1^{S\rightarrow A} & -\left(k_A^{1\rightarrow0} + k_S^{exc(0\rightarrow1)}\right) & k_S^{1\rightarrow0} & k_A^{2\rightarrow1} & 0 \\ 0 & 0 & k_S^{exc(0\rightarrow1)} & -\left(k_S^{1\rightarrow0} + k_A^{1\rightarrow0} + W_2^{S\rightarrow A}\right) & 0 & k_A^{2\rightarrow1} \\ 0 & 0 & 0 & W_2^{S\rightarrow A} & -\left(k_A^{2\rightarrow0} + k_A^{2\rightarrow1} + k_S^{exc(0\rightarrow1)}\right) & k_S^{1\rightarrow0} \\ 0 & 0 & 0 & 0 & k_S^{exc(0\rightarrow1)} & -\left(k_A^{2\rightarrow0} + k_A^{2\rightarrow1} + k_S^{1\rightarrow0}\right) \end{pmatrix}$$

**Figures S17** a) Complete kinetic scheme for modeling the energy transfer upconversion (ETU) processes occurring upon off-resonance irradiation into the sensitizer-centred absorption bands of a discrete SA dinuclear molecule, and b) associated kinetic matrix  $\mathbf{M}$  used in eq. (8).



**Figures S18** a) Complete kinetic scheme for modeling the energy transfer upconversion (ETU) processes occurring upon off-resonance irradiation into the sensitizer-centred absorption bands of a discrete SAS trinuclear molecule, and b) associated kinetic matrix  $\mathbf{M}$  used in eq. (8).

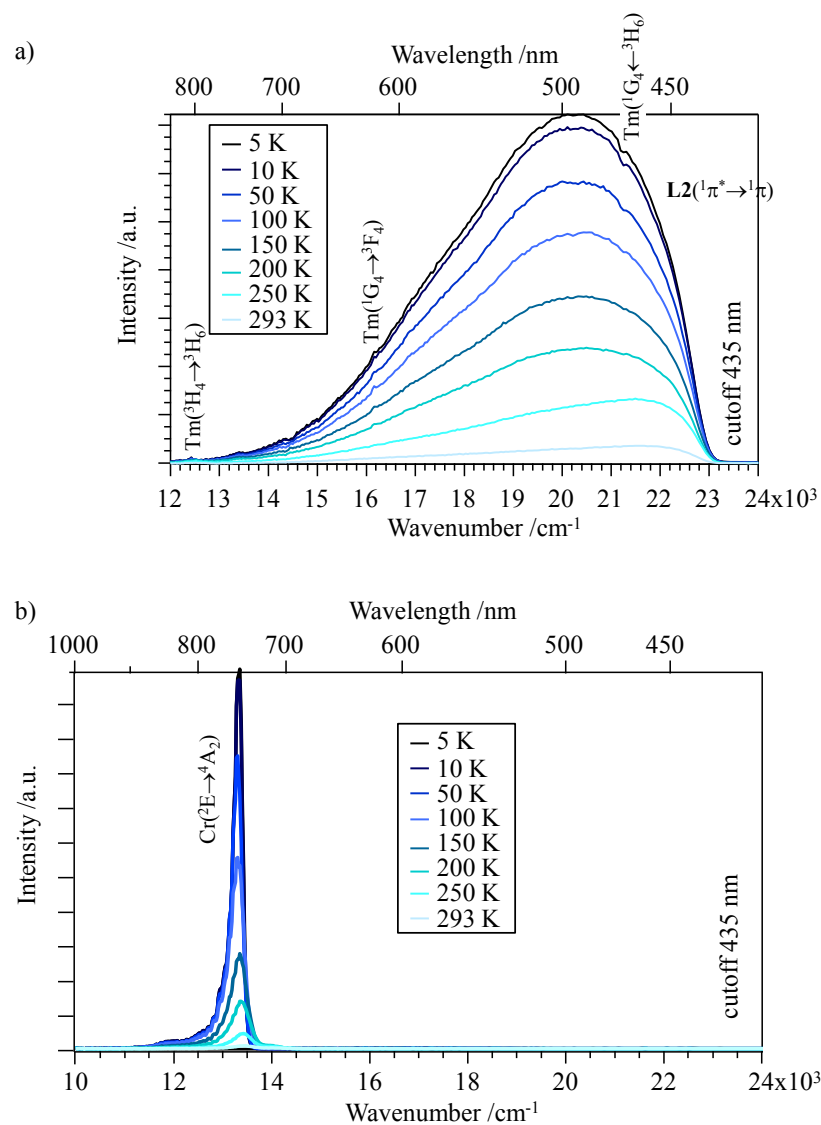


**Figure S19** Solid-state emission spectra of (a)  $[GaTmGa(L2)_3](CF_3SO_3)_9$  and (b)  $[CrTmCr(L2)_3](CF_3SO_3)_9$  at variable temperature ( $\tilde{\nu}_{exc} = 24691 \text{ cm}^{-1}$  or  $\lambda_{exc} = 405 \text{ nm}$ ). The dips correspond to internal Tm-centred re-absorption of ligand-centred emission.

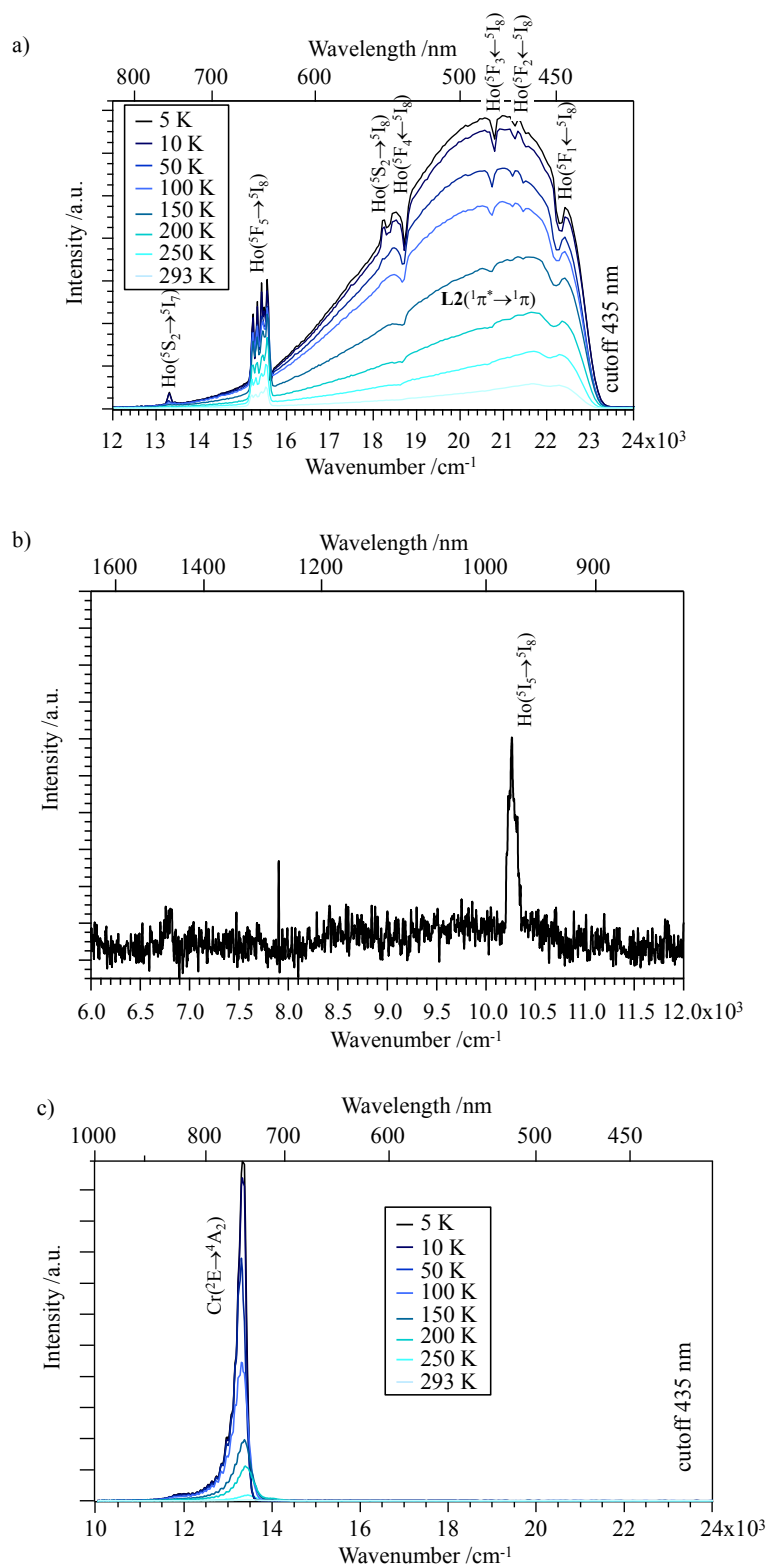


**Figure S20** Solid-state emission spectra of (a)-(b)  $[\text{GaHoGa}(\mathbf{L2})_3](\text{CF}_3\text{SO}_3)_9$  and (c)  $[\text{CrHoCr}(\mathbf{L2})_3](\text{CF}_3\text{SO}_3)_9$  at variable temperature ( $\tilde{\nu}_{\text{exc}} = 24691 \text{ cm}^{-1}$  or  $\lambda_{\text{exc}} = 405 \text{ nm}$ ). The dips correspond to internal Ho-centred re-absorption of ligand-centred emission.

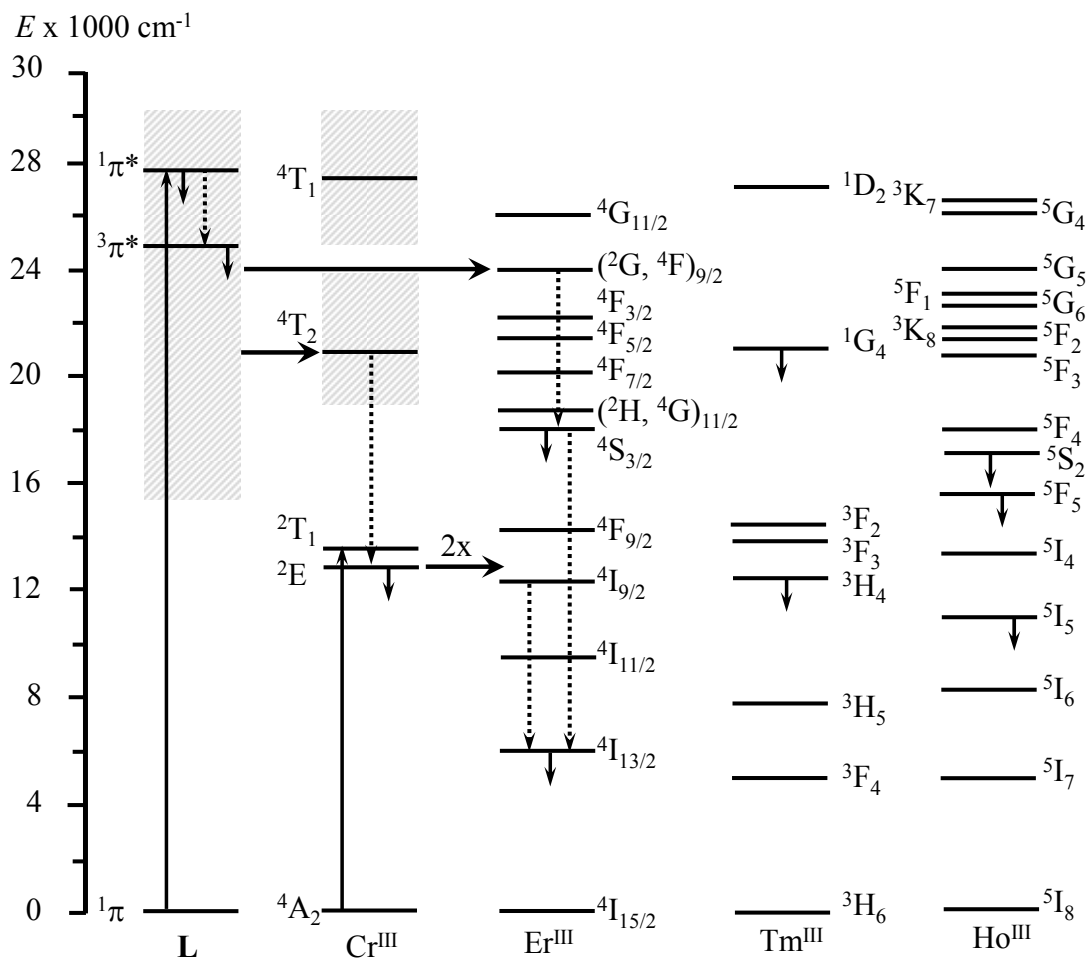


**Figure S21** Global Jablonski diagrams obtained from absorption and emission spectra recorded for the different chromophores in  $[\text{GaLnGa}(\mathbf{L2})_3](\text{CF}_3\text{SO}_3)_9$  and  $[\text{CrLnCr}(\mathbf{L2})_3](\text{CF}_3\text{SO}_3)_9$  ( $\text{Ln} = \text{Ho}, \text{Er}, \text{Tm}$ ). Upward full arrows indicate excitation processes. Downward full arrows correspond to emissive excited levels. Downward dashed arrows stand for internal conversion processes and horizontal arrows show intramolecular sensitizer-to-activator energy transfer processes occurring in CrErCr.

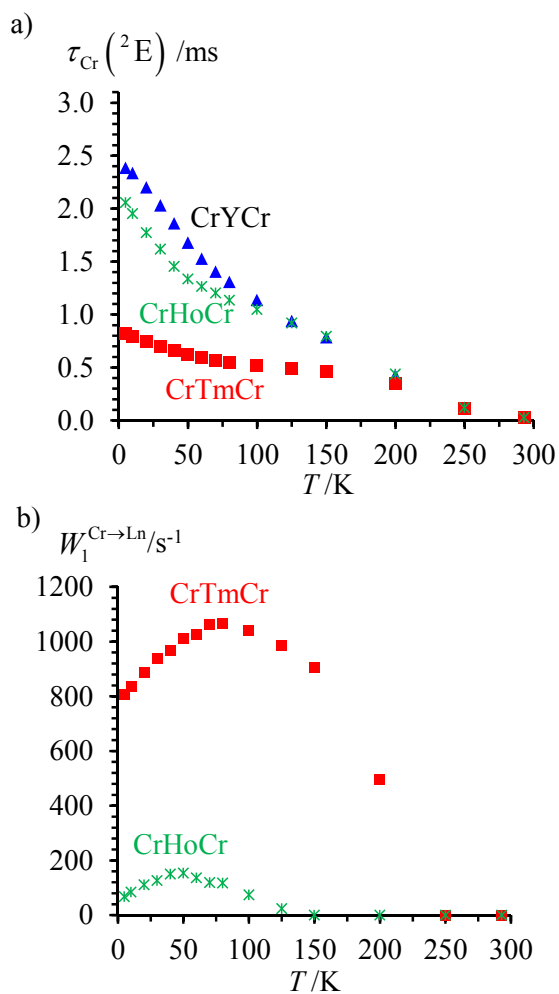


**Figure S22** a) Characteristic Cr(<sup>2</sup>E) lifetimes measured for [CrLnCr(L2)<sub>3</sub>](CF<sub>3</sub>SO<sub>3</sub>)<sub>9</sub> and b) associated rate constants computed with eq. (5) for the Cr(<sup>2</sup>E)→Tm(<sup>3</sup>H<sub>4</sub>) and Cr(<sup>2</sup>E)→Ho(<sup>5</sup>I<sub>5</sub>) energy transfer processes at various temperatures (Ln = Y, Ho, Tm; solid state 100%,  $\tilde{\nu}_{exc} = 28169 \text{ cm}^{-1}$  or  $\lambda_{exc} = 355 \text{ nm}$ ).

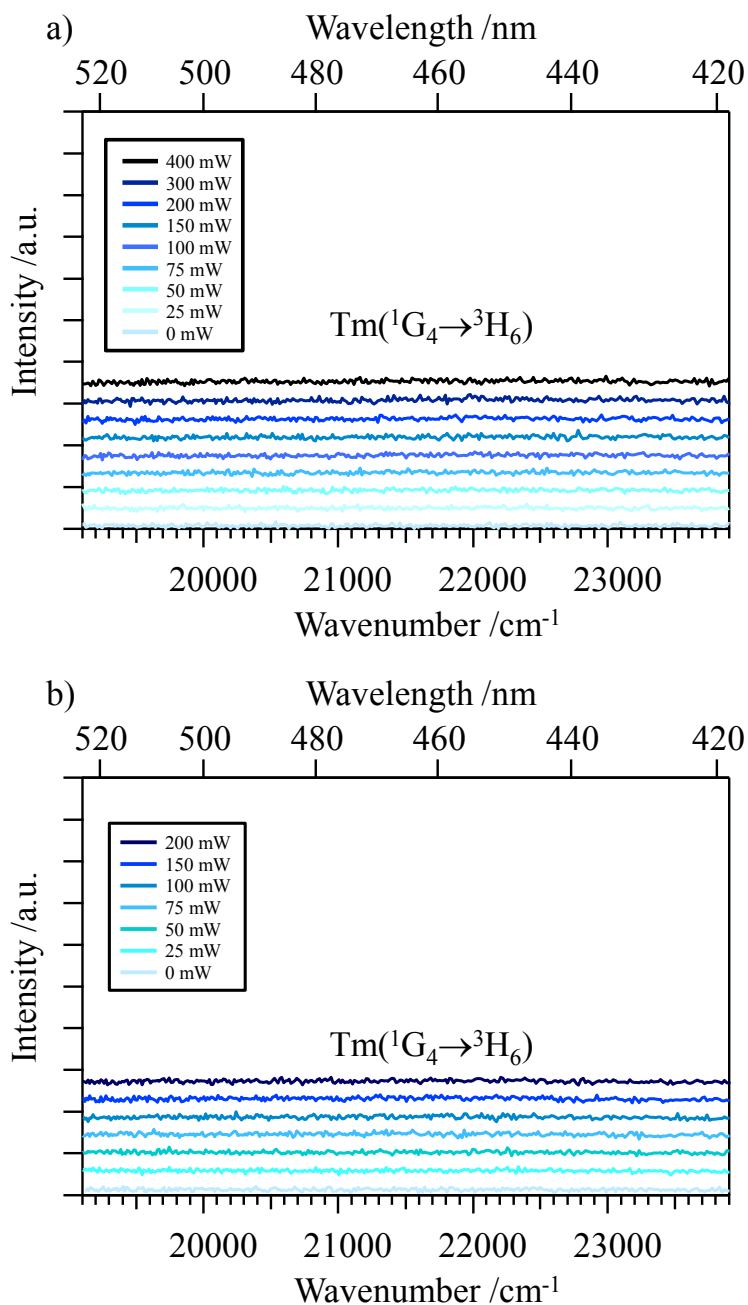


**Figure S23** Attempts to induce upconversion emission upon continuous-wave irradiation of a) the  $\text{Cr}(^2\text{E} \leftarrow ^4\text{A}_2)$  transition ( $\tilde{\nu}_{\text{exc}} = 13477 \text{ cm}^{-1}$  or  $\lambda_{\text{exc}} = 742 \text{ nm}$ ) and b) the  $\text{Cr}(^2\text{T}_1 \leftarrow ^4\text{A}_2)$  transition ( $\tilde{\nu}_{\text{exc}} = 14184 \text{ cm}^{-1}$  or  $\lambda_{\text{exc}} = 705 \text{ nm}$ ) in  $[\text{CrTmCr}(\text{L2})_3](\text{CF}_3\text{SO}_3)_9$  at variable power intensities (solid state, 30-33K, the excitation beam was loosely focused on the sample with a 100 mm lens).

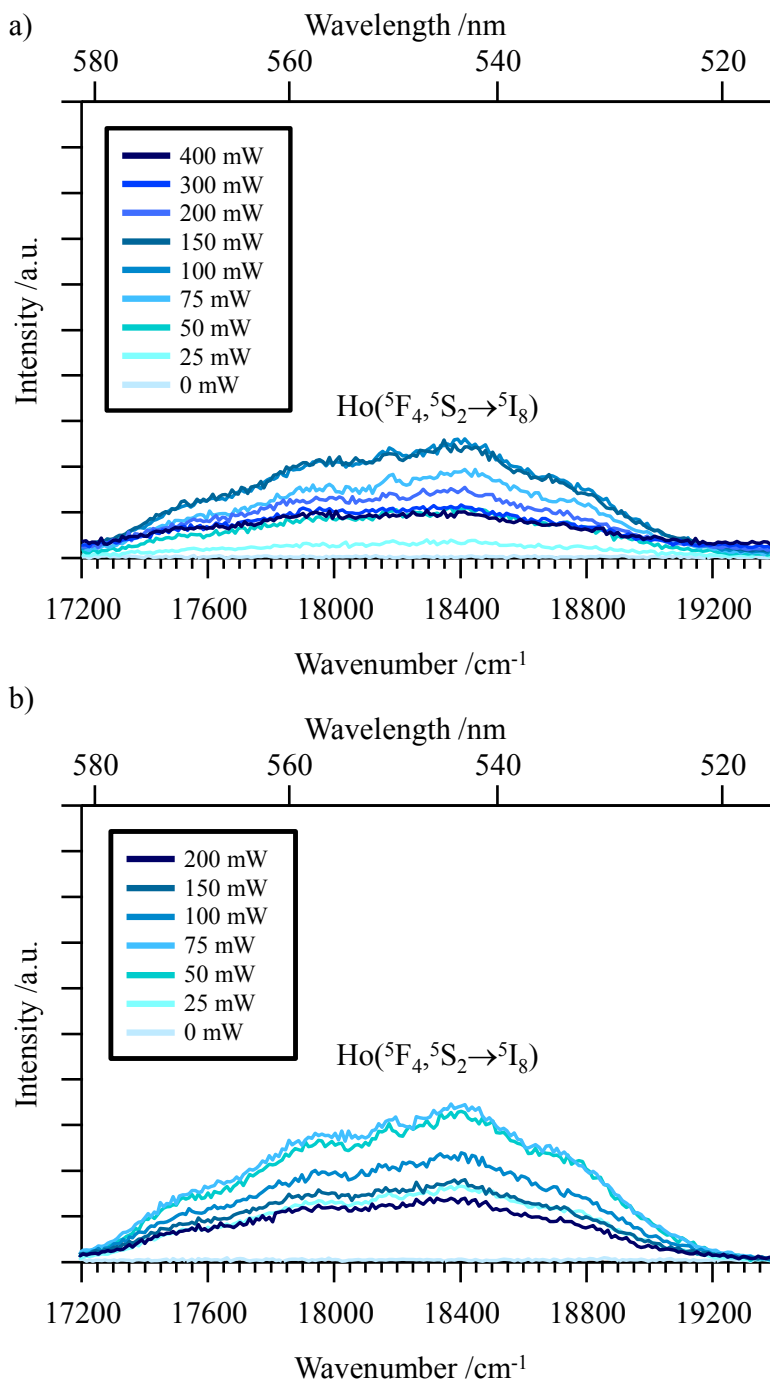


**Figure S24** Attempts to induce upconversion emission upon continuous-wave irradiation of a) the  $\text{Cr}(^2\text{E} \leftarrow ^4\text{A}_2)$  transition ( $\tilde{\nu}_{\text{exc}} = 13477 \text{ cm}^{-1}$  or  $\lambda_{\text{exc}} = 742 \text{ nm}$ ) and b) the  $\text{Cr}(^2\text{T}_1 \leftarrow ^4\text{A}_2)$  transition ( $\tilde{\nu}_{\text{exc}} = 14184 \text{ cm}^{-1}$  or  $\lambda_{\text{exc}} = 705 \text{ nm}$ ) in  $[\text{CrHoCr}(\text{L}2)_3](\text{CF}_3\text{SO}_3)_9$  at variable power intensities (solid state, 30-33K, the excitation beam was loosely focused on the sample with a 100 mm lens).

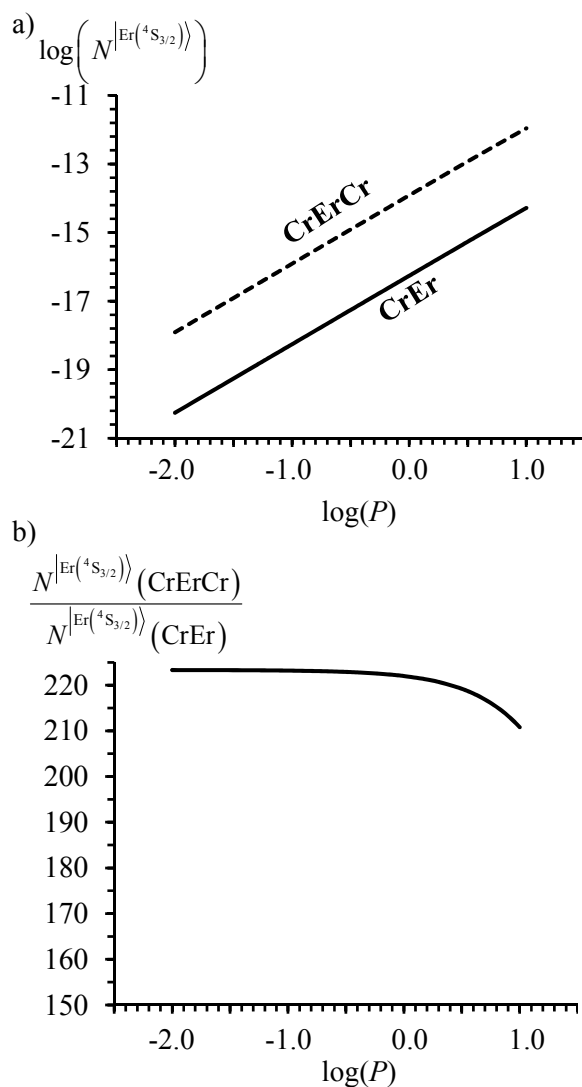


**Figure S25** a) Log-log plot and b) ratio of the quadratic dependence of the steady-state normalized population densities  $N^{|\text{Er}(^4\text{S}_{3/2})\rangle}$  on the incident pump intensity ( $P$  in  $\text{W}/\text{mm}^2$ ) computed for the dinuclear  $[\text{CrEr}(\mathbf{L1})_3](\text{CF}_3\text{SO}_3)_6$  (full trace) and for the trinuclear  $[\text{CrErCr}(\mathbf{L2})_3](\text{CF}_3\text{SO}_3)_9$  (dotted trace) complexes using eq. (9) and the kinetic rate constants gathered in Table 1.  $\sigma_{\text{Cr}}^{0 \rightarrow 1}(\text{CrEr}) \approx \sigma_{\text{Cr}}^{0 \rightarrow 1}(\text{CrErCr}) = 10^{-24} \text{ m}^2$ ,  $W_2^{\text{Cr} \rightarrow \text{Er}}(\text{CrEr}) = W_1^{\text{Cr} \rightarrow \text{Er}}(\text{CrEr}) = W_2^{\text{Cr} \rightarrow \text{Er}}(\text{CrErCr}) = W_1^{\text{Cr} \rightarrow \text{Er}}(\text{CrErCr}) = 170 \text{ s}^{-1}$ .